




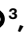



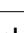












Ultrasensitive ctDNA detection for preoperative disease stratification in early-stage lung adenocarcinoma

Received: 21 September 2023

Accepted: 29 July 2024

Published online: 13 January 2025

 Check for updates

James R. M. Black ^{1,2,112}, Gabor Bartha^{3,112}, Charles W. Abbott³, Sean M. Boyle ³, Takahiro Karasaki ^{1,2,4,5}, Bailiang Li ³, Rui Chen ³, Jason Harris³, Selvaraju Veeriah¹, Martina Colopi¹, Maise Al Bakir ^{1,2}, Wing Kin Liu¹, John Lyle³, Fábio C. P. Navarro ³, Josette Northcott³, Rachel Marty Pyke³, Mark S. Hill ^{1,2}, Kerstin Thol^{1,6}, Ariana Huebner^{1,2,6}, Chris Bailey^{1,2}, Emma C. Colliver ^{1,2}, Carlos Martínez-Ruiz ^{1,6}, Kristiana Grigoriadis ^{1,2,6}, Piotr Pawlik^{1,6}, David A. Moore^{1,2,7}, Daniele Marinelli ^{1,6,8}, Oliver G. Shutkever¹, Cian Murphy ^{1,2}, Monica Sivakumar¹, TRACERx consortium*, Jacqui A. Shaw⁹, Allan Hackshaw ¹⁰, Nicholas McGranahan ^{1,6}, Mariam Jamal-Hanjani ^{1,4,11}, Alexander M. Frankell ^{1,2}, Richard O. Chen ^{3,113} & Charles Swanton ^{1,2,11,113} 

Circulating tumor DNA (ctDNA) detection can predict clinical risk in early-stage tumors. However, clinical applications are constrained by the sensitivity of clinically validated ctDNA detection approaches. NeXT Personal is a whole-genome-based, tumor-informed platform that has been analytically validated for ultrasensitive ctDNA detection at 1–3 ppm of ctDNA with 99.9% specificity. Through an analysis of 171 patients with early-stage lung cancer from the TRACERx study, we detected ctDNA pre-operatively within 81% of patients with lung adenocarcinoma (LUAD), including 53% of those with pathological TNM (pTNM) stage I disease. ctDNA predicted worse clinical outcome, and patients with LUAD with <80 ppm preoperative ctDNA levels (the 95% limit of detection of a ctDNA detection approach previously published in TRACERx) experienced reduced overall survival compared with ctDNA-negative patients with LUAD. Although prospective studies are needed to confirm the clinical utility of the assay, these data show that our approach has the potential to improve disease stratification in early-stage LUADs.

Liquid biopsy for detecting circulating tumor DNA (ctDNA, namely cell-free DNA derived from a tumor) holds promise as a strategy for personalized clinical management of early-stage cancers^{1–7}. Preoperative ctDNA status has shown potential as a biomarker, while postoperative ctDNA detection can direct adjuvant therapy regimens^{8,9}, and monitoring for molecular residual disease (MRD) during follow-up has the potential to identify relapse earlier than would be detected with routine clinical surveillance^{1,2,5,10}.

ctDNA detection can be tumor-informed or tumor-agnostic. Tumor-informed approaches leverage information from genomic profiling of a tumor tissue specimen, allowing for tracking of tumor-specific mutations within plasma and typically improving sensitivity relative to tumor-agnostic approaches. In 2020, cancer personalized profiling by deep sequencing (CAPP-seq), was used in a tumor-informed approach to demonstrate that preoperative ctDNA detection in non-small-cell lung cancer (NSCLC) could be used to

A full list of affiliations appears at the end of the paper. ✉ e-mail: Charles.swanton@crick.ac.uk

identify patients with stage I disease with poor clinical outcome¹¹. Subsequent work within lung adenocarcinomas (LUADs) from the LUNGCA-1 cohort¹², the NADIM trial¹³ and the TRACERx study¹ of NSCLC confirmed the prognostic capacity of preoperative ctDNA detection for overall survival (OS) and relapse-free survival (RFS) in LUADs.

Detection of preoperative ctDNA in early-stage LUAD is a considerable challenge owing to the low levels of ctDNA in plasma, which are frequently below 100 ppm^{10,14}. Additionally, the sensitivity of ctDNA detection can be impaired by variations in the production of cell-free DNA (cfDNA) by non-malignant cells¹⁵, sequencing error and variants arising from clonal hematopoiesis of indeterminate potential (CHIP), which can be present at low levels in plasma¹⁶. A high-quality ctDNA detection platform must have a number of attributes for optimal clinical utility: it must be extremely sensitive, highly specific and applicable to a broad spectrum of tumors, and it must deliver results with small amounts of DNA input. To that end, there has recently been significant focus on research into developing approaches to overcome this problem^{6,17–20}.

Although the relationship between ctDNA detection and survival is independent of pathological tumor-node-metastasis (pTNM) stage in this setting, the degree to which the limit of detection (LOD) of ctDNA assays affects the clinical sensitivity of ctDNA as a biomarker for aggressive disease is not well understood.

Here, we used NeXT Personal, an ultrasensitive, tumor-informed liquid-biopsy platform to characterize preoperative ctDNA in 171 patients in the TRACERx study^{1,21,22}. NeXT Personal is a tumor-informed liquid-biopsy platform that leverages prioritized target selection from whole-genome sequencing of tumor and matched normal DNA²³. The development and analytical validation of this assay is outlined in Methods and in ref. 23. In brief, the method aims to achieve a LOD approaching 1 ppm by aggregating the signal from a larger number of somatic variant targets than can be detected from an exome. To avoid being overwhelmed by false signals arising from the large number of variants, noise must be suppressed to very low levels, which is largely accomplished by molecular consensus, which allows identification of independent sequence reads arising from a common founder, and groups these reads into unique molecule families for further analysis. NeXT Personal bespoke panels are designed using the top ~1,800 signal-to-noise ranked somatic variants for ctDNA detection from plasma (that is, the subset of cfDNA that contains the tumor-specific mutations in the panel). Hybridization-based genomic-target enrichment using the panel is followed by ultradeep sequencing of the plasma samples. NeXT Personal then aggregates the tumor-derived signal from the somatic targets. This process, combined with comprehensive noise-suppression methods, enables NeXT Personal to achieve ultrasensitive ctDNA detection for disease stratification, therapy monitoring and MRD detection (Methods and Fig. 1a).

Personalized tumor-informed ctDNA-detection assays that leverage exonic mutations have been investigated in the TRACERx cohort^{1,2}. We have previously studied the ability of ctDNA, detected in a preoperative peripheral blood sample, to predict clinical outcome in LUAD¹. This involved a tumor-informed assay investigating somatic variants at an average of 200 positions per sample, revealing that patients with LUAD who had ctDNA detected in their blood at the time of surgery had a worse clinical prognosis²⁴. However, ctDNA was detectable in only 14% of patients with pathological stage I LUAD at this time point. We therefore set out to assess the degree to which a more sensitive and specific assay would increase prognostic value in a cohort with comparable clinical demographics (Extended Data Table 1).

We analyzed blood plasma samples collected before the surgical removal of lung cancer from 171 TRACERx patients, including 94 with LUAD (29.8% stage I, 30.9% stage II, 39.3% stage III) and 77 with non-LUAD (28.6% stage I, 40.3% stage II, 31.2% stage III) NSCLC, using NeXT Personal (Extended Data Table 2 and Fig. 1b). Of these patients, 160 had one primary NSCLC tumor and 11 had two synchronous primary

NSCLC tumors. A median of 1,800 patient-specific somatic variants were included in the NeXT Personal panel design (range, 646–1,942), of which a median of 97.83% were from non-coding regions (Extended Data Fig. 1a). This resulted in a set of bespoke panels with a median predicted LOD of 1.33 ppm and a range of 0.85–4.45 ppm (Extended Data Fig. 1b). The median DNA input quantity was 23.5 ng (Fig. 1b; range, 4.01–50.0 ng).

ctDNA was detected in a preoperative plasma sample in 81% of patients with LUAD (Fig. 1c, 76/94) and 100% of patients with non-LUAD (Fig. 1d, 77/77) NSCLCs across a broad range of tumor fractions (positive ctDNA detection range, 1.66–253,826 ppm). This included 32 LUADs (34% of all LUADs) in which ctDNA was detected, but at below 80 ppm, the 95% LOD in our previous approach². We could detect ctDNA in the blood of 57% of patients with pTNM stage I LUADs (16/28): ctDNA from these tumors has been difficult to detect in blood samples (only 14% of such tumors were identified in Abbosh et al.² and 13% in Abbosh et al.¹). Similarly, ctDNA was detected in 79% of pTNM stage II LUADs (23/29, compared to 44% in Abbosh et al.²). ctDNA shedding, as previously reported, was associated with smoking status (pack-year history) (Spearman's $\rho = 0.18$, $P = 0.021$; Extended Data Fig. 1c)² and with the high-grade predominant subtypes of LUAD, in particular the solid and cribriform subtypes ($P = 1.3 \times 10^{-8}$, Kruskal–Wallis test; Extended Data Fig. 1d)²⁵. Oncogenic events, which in this cohort comprised *EGFR* mutations and skipping of *MET* exon 14 (no RET–ROS1–ALK oncogenic fusions were detected), were not associated with a significant difference in ctDNA ppm level ($P = 0.23$, Kruskal–Wallis test; Extended Data Fig. 1e) or rate of preoperative ctDNA detection ($P = 0.16$, Fisher's exact test; Extended Data Fig. 1f), although this analysis is likely to have been underpowered given the small numbers of patients harboring these events.

We next assessed the degree to which this additional sensitivity improved our ability to stratify these patients according to clinical outcome. Preoperative ctDNA-negative patients were compared with patients whose ctDNA levels were below the median of those detected (ctDNA-low) and those with ctDNA levels above the median of those detected (ctDNA high). ctDNA status predicted OS in LUADs (Fig. 2a, low: hazard ratio (HR) = 11.08, 95% confidence interval (CI) = 1.48–83.2; high: HR = 19.33, 95% CI = 2.56–146.0) and RFS (Extended Data Fig. 2a, low: HR = 14.17, 95% CI = 1.91–105.3; high: HR = 25.79, 95% CI = 3.48–191.4). Patients with a preoperative ctDNA-negative status had significantly improved OS (5-year OS, 100%; 95% CI = 100%–100%; $n = 18$) compared with ctDNA-low patients (5-year OS, 61.4%; 95% CI = 47.3%–79.6%; $n = 38$), and ctDNA-high patients (5-year OS, 48.8%; 95% CI = 34.7%–68.7%; $n = 38$). Notably, when analysis was restricted to include only patients in whom ctDNA would not have been reliably detected using the approach in Abbosh et al.², the presence of ctDNA at levels below 80 ppm remained prognostic for poor OS (Fig. 2b, $P = 0.0029$; HR = 12.33; 95% CI = 1.63–93.35) and RFS (Extended Data Fig. 2b, $P = 0.00011$; HR = 18.07; 95% CI = 2.41–135.3) in LUAD. This suggests that clinically meaningful signal is detected by assays with sensitivity at tumor fractions below 80 ppm, and that the ultra-high-sensitivity assay presented here enables identification of a group of very-low-risk patients with LUAD.

As we have previously reported, the association between outcomes and elevated preoperative ctDNA levels in non-LUADs was substantially reduced compared with that in LUADs; previous work has found no discernible impact of ctDNA levels on clinical outcome in non-LUADs¹. In this analysis, a ctDNA level greater than the median in non-LUADs was not associated with reduced RFS (Extended Data Fig. 2c; HR = 1.81; 95% CI = 0.93–3.92; $P = 0.077$). This highlights a fundamentally different relationship between ctDNA and disease biology in non-LUADs compared with that in LUADs.

When adjusted for histology, pTNM stage, smoking status, age, the presence of an oncogenic event (such as an *EGFR* driver mutation or the skipping of exon 14 in *MET*) and the addition of adjuvant therapy,

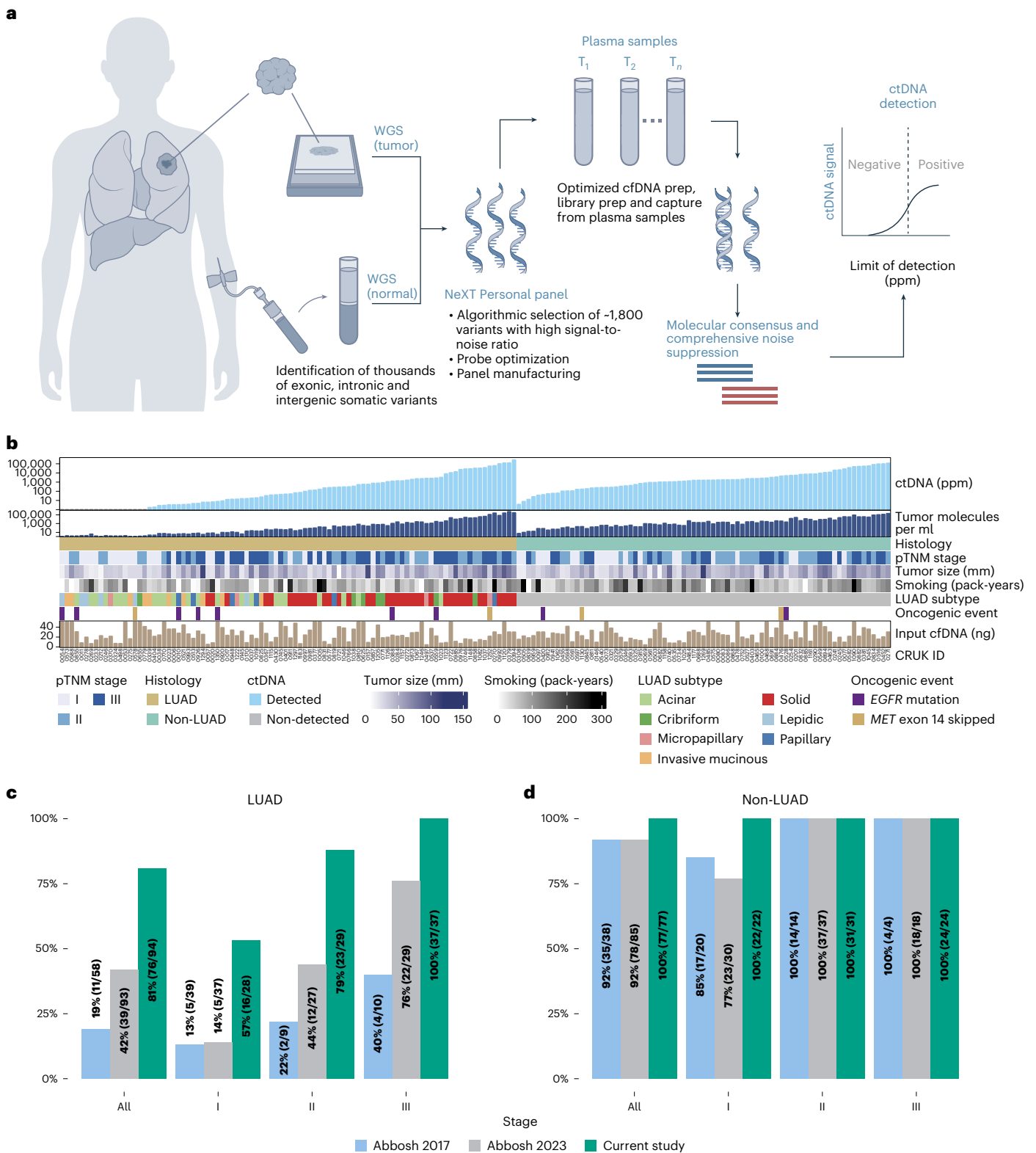


Fig. 1 | Highly sensitive detection of preoperative ctDNA. a, The NeXT Personal platform leverages tumor-informed information to achieve ultrasensitive and specific residual and recurrent cancer detection, longitudinal monitoring and therapy monitoring from liquid-biopsy samples. **b**, Clinicopathological variables relating to preoperative ctDNA detection in patients with NSCLC in the TRACERx study: ctDNA level (ppm tumor fraction); number of tumor molecules per ml plasma; pathological tumor node metastasis (pTNM) stage; NSCLC histology;

tumor size (pathology-based tumor size (mm)); cigarette smoking (pack-years); pathological subtype of LUAD; presence of an oncogenic event (within this cohort, either the presence of an EGFR mutation or skipping of MET exon 14); and cfDNA input amount (ng). *n* = 171. **c, d**, Fraction of TRACERx LUAD (**c**) and non-LUAD (**d**) tumors detected pre-operatively. Colors represent different studies: blue, Abbosh et al.¹; gray, Abbosh et al.²; green, this study. *n* = 94 LUAD, *n* = 77 non-LUAD.

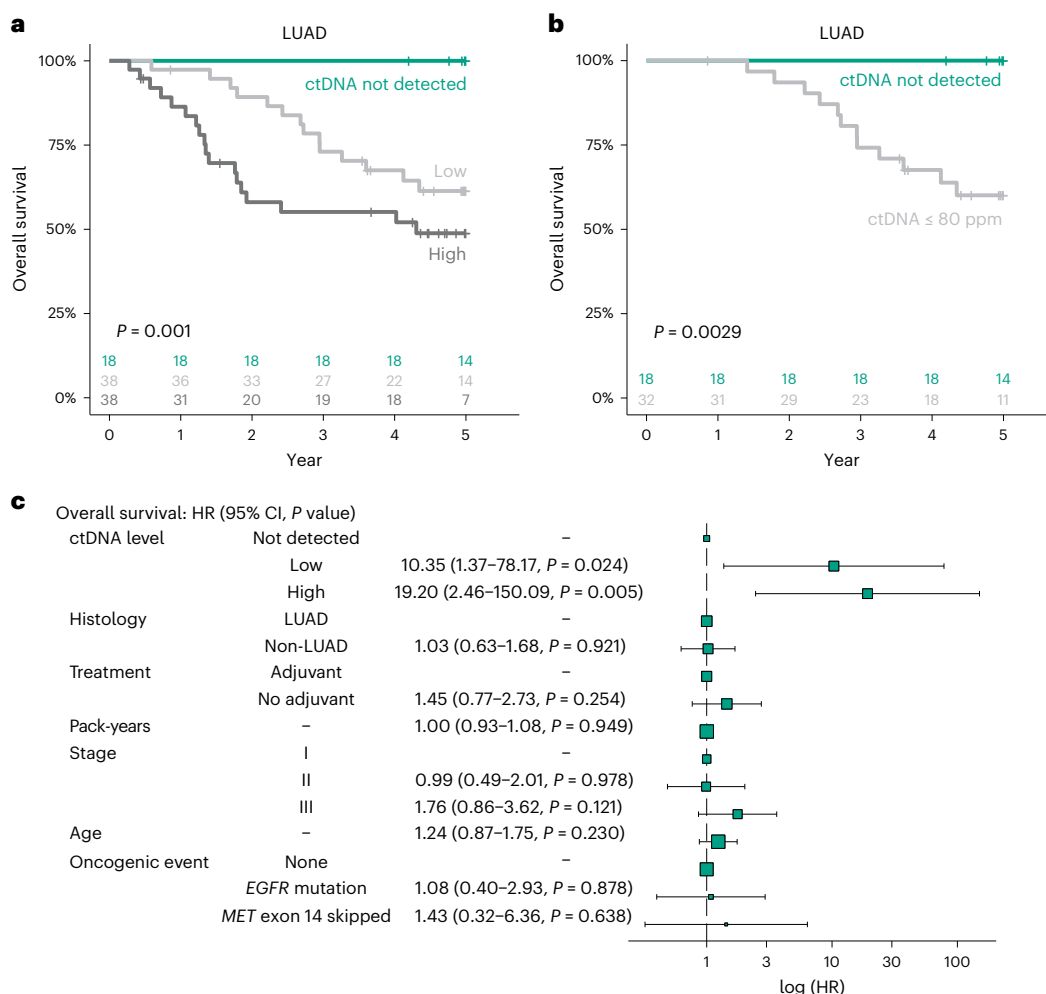


Fig. 2 | Baseline ctDNA level is prognostic of OS. a, Kaplan–Meier (KM) curve of OS in ctDNA-high (dark gray), ctDNA-low (light gray) and ctDNA-negative (green) patients with LUAD. ctDNA-high and ctDNA-low groups were defined according to the median ctDNA levels across ctDNA-positive LUADs. P values were calculated using log-rank tests. **b**, KM curve demonstrating OS in patients harboring ctDNA at an estimated tumor fraction below the limit of reliable detection described in Abbosh et al.² (light gray) and ctDNA-negative patients (green). P values were calculated using log-rank tests. **c**, Results of multivariable

Cox regression analysis including ctDNA level (ctDNA-high, ctDNA-low, ctDNA-negative); histology; whether the patient received adjuvant chemotherapy; cigarette smoking history (in increments of 10 pack-years); pTNM stage; age (in increments of 10 years); and the presence of an oncogenic event (either an *EGFR* mutation or *MET* exon 14 skipping). $n = 171$. Error bars represent 95% confidence intervals. The size of the boxes represent the number of patients within each category.

the presence of ctDNA—whether considered either as a continuous metric or stratified into groups as specified above—was independently associated with reduced OS (Fig. 2c and Extended Data Fig. 3a) and RFS (Extended Data Fig. 3b,c) in a pooled cohort of patients with LUADs and non-LUADs. Of note, the ctDNA level was not significant as an independent prognostic factor for RFS in the non-LUAD group (Extended Data Fig. 3d,e). The prognostic effect of ctDNA as a continuous variable on both RFS and OS was not significant when adjusting for histological (squamous versus non-squamous) subtype and other clinicopathological factors (Extended Data Fig. 3f,g).

This work has leveraged NeXT Personal, a tumor-informed assay that is capable of reliably detecting ctDNA in blood at 1–3 ppm (0.0001–0.0003% tumor fraction). Notably, this ultra-high sensitivity can be achieved with an estimated specificity of 99.9% and even from suboptimal DNA input volumes. This could be important in many clinical settings, and can be applied to suboptimal DNA input volumes.

Patients with early-stage NSCLC remain at high risk of relapse, despite aggressive curative-intent treatment. Thus, it is of critical importance to accurately stratify patients to both maximize the likelihood of disease cure following surgery and adjuvant therapy and

minimize risk of overtreatment in those patients predicted to have good outcome. Detectable preoperative ctDNA has been associated with worsened recurrence-free survival and reduced OS^{12,26,27}, and has been suggested as a potential marker for neoadjuvant treatment selection^{8,9}. We have demonstrated that assays that cannot detect ctDNA at tumor fractions below 80 ppm fail to capture a clinically impactful signal arising from a significant subset of patients with LUAD². In this study, these patients with detectable but extremely low levels of ctDNA experienced a worse clinical outcome than those in whom we did not detect evidence of ctDNA. This suggests that there is a subset of very-low-risk patients with LUADs who can be definitively identified only by using an ultrasensitive ctDNA assay, raising the potential for an ultrasensitive and specific assay to be used prognostically for escalation of therapy in stage I LUADs exhibiting ctDNA release.

Although this study presents results from preoperative plasma samples, the high sensitivity of the NeXT Personal assay suggests the potential for significant clinical benefit in the setting of minimal residual disease for tracking treatment response and detecting recurrence.

Of note, there are a number of technologies in the field aiming to achieve ultrasensitive tumor-informed ctDNA detection, such those

developed by Foresight Diagnostics (PhasED-seq)^{18,28}, C2i Genomics⁹ and Inivata (RaDaR)⁶.

This work has limitations. The data from TRACERx was analyzed retrospectively, although in a blinded fashion. Future data from prospective cohorts will be needed to evaluate the clinical utility of this assay. Although NeXT Personal is already in use as a clinical diagnostic test, it, like other tumor-informed ctDNA detection assays, is of higher complexity, can be more costly to produce and requires a longer turnaround period to develop the panel and obtain a clinically actionable result, compared with non-tumor-informed approaches.

If ctDNA is to be used for clinical risk prediction, the design of personalized adjuvant treatment regimens and early detection of recurrence and integrated into routine clinical care, ctDNA assays should have a high degree of sensitivity. In this way, they hold promise to transform adjuvant clinical trial design and clinical practice.

Online content

Any methods, additional references, Nature Portfolio reporting summaries, source data, extended data, supplementary information, acknowledgements, peer review information; details of author contributions and competing interests; and statements of data and code availability are available at <https://doi.org/10.1038/s41591-024-03216-y>.

References

- Abbosh, C. et al. Phylogenetic ctDNA analysis depicts early stage lung cancer evolution. *Nature* **545**, 446–451 (2017).
- Abbosh, C. et al. Tracking early lung cancer metastatic dissemination in TRACERx using ctDNA. *Nature* **616**, 553–562 (2023).
- Pascual, J. et al. ESMO recommendations on the use of circulating tumour DNA assays for patients with cancer: a report from the ESMO Precision Medicine Working Group. *Ann. Oncol.* **33**, 750–768 (2022).
- García-Murillas, I. et al. Mutation tracking in circulating tumor DNA predicts relapse in early breast cancer. *Sci. Transl. Med.* **7**, 302ra133 (2015).
- Reinert, T. et al. Analysis of plasma cell-free DNA by ultradeep sequencing in patients with stages I to III colorectal cancer. *JAMA Oncol.* **5**, 1124–1131 (2019).
- Gale, D. et al. Residual ctDNA after treatment predicts early relapse in patients with early-stage non-small cell lung cancer. *Ann. Oncol.* **33**, 500–510 (2022).
- Kotani, D. et al. Molecular residual disease and efficacy of adjuvant chemotherapy in patients with colorectal cancer. *Nat. Med.* **29**, 127–134 (2023).
- Powles, T. et al. ctDNA guiding adjuvant immunotherapy in urothelial carcinoma. *Nature* **595**, 432–437 (2021).
- Tie, J. et al. Circulating tumor DNA analysis guiding adjuvant therapy in stage II colon cancer. *N. Engl. J. Med.* **386**, 2261–2272 (2022).
- Chaudhuri, A. A. et al. Early detection of molecular residual disease in localized lung cancer by circulating tumor DNA profiling. *Cancer Discov.* **7**, 1394–1403 (2017).
- Chabon, J. J. et al. Integrating genomic features for non-invasive early lung cancer detection. *Nature* **580**, 245–251 (2020).
- Xia, L. et al. Perioperative ctDNA-based molecular residual disease detection for non-small cell lung cancer: a prospective multicenter cohort study (LUNGCA-1). *Clin. Cancer Res.* **28**, 3308–3317 (2022).
- Provencio, M. et al. Overall survival and biomarker analysis of neoadjuvant nivolumab plus chemotherapy in operable stage IIIA non-small-cell lung cancer (NADIM phase II trial). *J. Clin. Oncol.* **40**, 2924 (2022).
- Chin, R.-I. et al. Detection of solid tumor molecular residual disease (MRD) using circulating tumor DNA (ctDNA). *Mol. Diagn. Ther.* **23**, 311–331 (2019).
- Mattox, A. K. et al. The origin of highly elevated cell-free DNA in healthy individuals and patients with pancreatic, colorectal, lung, or ovarian cancer. *Cancer Discov.* **13**, 2166–2179 (2023).
- Hu, Y. et al. False-positive plasma genotyping due to clonal hematopoiesis. *Clin. Cancer Res.* **24**, 4437–4443 (2018).
- Cohen, J. D. et al. Detection of low-frequency DNA variants by targeted sequencing of the Watson and Crick strands. *Nat. Biotechnol.* **39**, 1220–1227 (2021).
- Kurtz, D. M. et al. Enhanced detection of minimal residual disease by targeted sequencing of phased variants in circulating tumor DNA. *Nat. Biotechnol.* **39**, 1537–1547 (2021).
- Zviran, A. et al. Genome-wide cell-free DNA mutational integration enables ultra-sensitive cancer monitoring. *Nat. Med.* **26**, 1114–1124 (2020).
- Cohen, J. D. et al. Detection and localization of surgically resectable cancers with a multi-analyte blood test. *Science* **359**, 926–930 (2018).
- Jamal-Hanjani, M. et al. Tracking the evolution of non-small-cell lung cancer. *N. Engl. J. Med.* **376**, 2109–2121 (2017).
- Martínez-Ruiz, C. et al. Genomic–transcriptomic evolution in lung cancer and metastasis. *Nature* **616**, 543–555 (2023).
- Northcott, J. et al. Analytical validation of NeXT Personal[®], an ultra-sensitive personalized circulating tumor DNA assay. *Oncotarget* **15**, 200–218 (2024).
- Zhao, J. et al. Personalized cancer monitoring assay for the detection of ctDNA in patients with solid tumors. *Mol. Diagn. Ther.* **27**, 753–768 (2023).
- Karasaki, T. et al. Evolutionary characterization of lung adenocarcinoma morphology in TRACERx. *Nat. Med.* **29**, 833–845 (2023).
- Jung, H.-A. et al. Longitudinal monitoring of circulating tumor DNA from plasma in patients with curative resected stages I to IIIA EGFR-mutant non-small cell lung cancer. *J. Thorac. Oncol.* **18**, 1199–1208 (2023).
- Li, N. et al. Perioperative circulating tumor DNA as a potential prognostic marker for operable stage I to IIIA non-small cell lung cancer. *Cancer* **128**, 708–718 (2022).
- Isbell, J. M. et al. Abstract 3375: ultrasensitive ctDNA minimal residual disease monitoring in early NSCLC with PhasED-Seq. *Cancer Res.* **83**, 3375 (2023).

Publisher's note Springer Nature remains neutral with regard to jurisdictional claims in published maps and institutional affiliations.

Open Access This article is licensed under a Creative Commons Attribution 4.0 International License, which permits use, sharing, adaptation, distribution and reproduction in any medium or format, as long as you give appropriate credit to the original author(s) and the source, provide a link to the Creative Commons licence, and indicate if changes were made. The images or other third party material in this article are included in the article's Creative Commons licence, unless indicated otherwise in a credit line to the material. If material is not included in the article's Creative Commons licence and your intended use is not permitted by statutory regulation or exceeds the permitted use, you will need to obtain permission directly from the copyright holder. To view a copy of this licence, visit <http://creativecommons.org/licenses/by/4.0/>.

© The Author(s) 2025

¹Cancer Research UK Lung Cancer Centre of Excellence, University College London Cancer Institute, London, UK. ²Cancer Evolution and Genome Instability Laboratory, The Francis Crick Institute, London, UK. ³Personalis Inc., Fremont, CA, USA. ⁴Cancer Metastasis Laboratory, University College London Cancer Institute, London, UK. ⁵Department of Thoracic Surgery, Respiratory Center, Toranomon Hospital, Tokyo, Japan. ⁶Cancer Genome Evolution Research Group, Cancer Research UK Lung Cancer Centre of Excellence, University College London Cancer Institute, London, UK. ⁷Department of Cellular Pathology, University College London Hospitals, London, UK. ⁸Department of Experimental Medicine, Sapienza University, Rome, Italy. ⁹Leicester NIHR BRC & University of Leicester, Leicester, UK. ¹⁰Cancer Research UK & UCL Cancer Trials Centre, London, UK. ¹¹Department of Oncology, University College London Hospitals, London, UK. ¹¹²These authors contributed equally: James R. M. Black, Gabor Bartha. ¹¹³These authors jointly supervised this work: Richard O. Chen, Charles Swanton. ✉e-mail: Charles.swanton@crick.ac.uk

TRACERx consortium

Charles Swanton^{1,2,11,113}, Alexander M. Frankell^{1,2}, Mariam Jamal-Hanjani^{1,4,11}, Nicholas McGranahan^{1,6}, Allan Hackshaw¹⁰, Jacqui A. Shaw⁹, James R. M. Black^{1,2,112}, Takahiro Karasaki^{1,2,4,5}, Selvaraju Veeriah¹, Maise Al Bakir^{1,2}, Wing Kin Liu¹, Mark S. Hill^{1,2}, Kerstin Thol^{1,6}, Ariana Huebner^{1,2,6}, Chris Bailey^{1,2}, Emma C. Colliver^{1,2}, Carlos Martínez-Ruiz^{1,6}, Kristiana Grigoriadis^{1,2,6}, Piotr Pawlik^{1,6}, David A. Moore^{1,2,7}, Monica Sivakumar¹, Jason F. Lester¹², Amrita Bajaj¹³, Apostolos Nakas¹³, Azmina Sodha-Ramdeen¹³, Mohamad Tufail¹³, Molly Scotland¹³, Rebecca Boyles¹³, Sridhar Rathinam¹³, Claire Wilson¹⁴, Domenic Marrone¹⁵, Sean Dooloo^{13,15}, Dean A. Fennell^{13,15}, Gurdeep Matharu¹⁶, Ekaterini Boleti¹⁷, Heather Cheyne¹⁸, Mohammed Khalil¹⁸, Shirley Richardson¹⁸, Tracey Cruickshank¹⁸, Gillian Price^{19,20}, Keith M. Kerr^{20,21}, Sarah Benafif^{11,22}, Jack French²², Kayleigh Gilbert²², Babu Naidu²³, Akshay J. Patel²⁴, Aya Osman²⁵, Carol Enstone²⁵, Gerald Langman²⁵, Helen Shackelford²⁵, Madava Djearaman²⁵, Salma Kadiri²⁵, Gary Middleton^{25,26}, Angela Leek²⁷, Jack Davies Hodgkinson²⁷, Nicola Totton²⁷, Angeles Montero²⁸, Elaine Smith²⁸, Eustace Fontaine²⁸, Felice Granato²⁸, Antonio Paiva-Correia²⁹, Juliette Novasio²⁸, Kendadai Rammohan²⁸, Leena Joseph²⁸, Paul Bishop²⁸, Rajesh Shah²⁸, Stuart Moss²⁸, Vijay Joshi²⁸, Philip A. J. Crosbie^{28,30,31}, Katherine D. Brown^{31,32}, Mathew Carter^{31,32}, Anshuman Chaturvedi^{31,32}, Pedro Oliveira^{31,32}, Colin R. Lindsay^{31,33}, Fiona H. Blackhall^{31,33}, Matthew G. Krebs³³, Yvonne Summers^{31,33}, Alexandra Clipson^{31,34}, Jonathan Tugwood^{31,34}, Alastair Kerr^{31,34}, Dominic G. Rothwell^{31,34}, Caroline Dive^{31,34}, Hugo JWL Aerts^{35,36,37}, Roland F. Schwarz^{38,39}, Tom L. Kaufmann^{39,40}, Gareth A. Wilson², Rachel Rosenthal², Peter Van Loo^{41,42,43}, Nicolai J. Birkbak^{1,2,44,45,46}, Zoltan Szallasi^{47,48,49}, Judit Kisistok^{44,45,46}, Mateo Sokac^{44,45,46}, Roberto Salgado^{50,51}, Miklos Diossy^{47,48,52}, Jonas Demeulemeester^{53,54,55}, Abigail Bunkum^{1,4,56}, Angela Dwornik⁵⁷, Alastair Magness⁵⁸, Andrew J. Rowan², Angeliki Karamani⁵⁷, Antonia Toncheva¹, Benny Chain⁵⁷, Carla Castignani^{43,59}, Christopher Abbosh¹, Clare Puttick^{1,2,6}, Clare E. Weeden⁵⁸, Claudia Lee², Corentin Richard¹, Crispin T. Hiley^{1,2}, Cristina Naceur-Lombardelli¹, David R. Pearce⁵⁷, Despoina Karagianni⁵⁷, Dhruva Biswas^{1,2,60}, Dina Levi⁵⁸, Elizabeth Larose Cadieux^{43,59}, Emilia L. Lim^{1,2}, Emma Nye⁶¹, Eva Grönroos⁵⁸, Felip Gálvez-Cancino⁵⁷, Francisco Gimeno-Valiente¹, George Kassiotis^{58,62}, Georgia Stavrou⁵⁷, Gerasimos-Theodoros Mastrokalos⁵⁷, Helen L. Lowe⁵⁷, Ignacio Garcia Matos⁵⁷, Imran Noorani⁵⁸, Jacki Goldman⁵⁸, James L. Reading⁵⁷, Jayant K. Rane^{2,57}, Jerome Nicod⁶³, John A. Hartley⁵⁷, Karl S. Peggs^{64,65}, Katey S. S. Enfield², Kayalvizhi Selvaraju⁵⁷, Kevin Litchfield^{1,66}, Kevin W. Ng⁶⁷, Kezhong Chen⁵⁷, Krijn Dijkstra⁵⁸, Krupa Thakkar¹, Leah Ensell⁵⁷, Mansi Shah⁵⁷, Maria Litovchenko⁵⁷, Mariana Werner Sunderland¹, Matthew R. Huska⁶⁸, Michelle Dietzen^{1,2,6}, Michelle M. Leung^{1,2,6}, Mickael Escudero⁵⁸, Mihaela Angelova², Miljana Tanić^{59,69}, Nnennaya Kanu¹, Olga Chervova^{57,70}, Olivia Lucas^{1,2,56,71}, Oriol Pich², Othman Al-Sawaf^{65,72}, Paulina Prymas¹, Philip Hobson⁵⁸, Richard Kevin Stone⁶¹, Robert Bentham^{1,6}, Robert E. Hynds⁵⁷, Roberto Vendramin^{1,2,66}, Sadegh Saghafinia¹, Samuel Gamble⁵⁷, Seng Kuong Anakin Ung⁵⁷, Sergio A. Quezada^{1,73}, Sharon Vanloo¹, Simone Zaccaria^{1,56}, Sonya Hessey^{1,4,56}, Sophia Ward^{1,2,63}, Sian Harries^{1,2,63}, Stefan Boeing⁵⁸, Stephan Beck⁵⁹, Supreet Kaur Bola⁵⁷, Tamara Denner⁵⁸, Teresa Marafioti⁷, Thomas B. K. Watkins^{57,74}, Thomas Patrick Jones⁶, Victoria Spanswick⁵⁷, Vittorio Barbé⁵⁸, Wei-Ting Lu⁵⁸, William Hill⁵⁸, Yin Wu⁵⁷, Yutaka Naito⁵⁸, Zoe Ramsden⁵⁸, Catarina Veiga⁷⁵, Gary Royle⁷⁶, Charles-Antoine Collins-Fekete⁷⁷, Francesco Fraioli⁷⁸, Paul Ashford⁷⁹, Martin D. Forster^{1,11}, Siow Ming Lee^{1,11}, Elaine Borg⁷, Mary Falzon⁷, Dionysis Papadatos-Pastos¹¹, James Wilson¹¹, Tanya Ahmad¹¹, Alexander James Procter⁸⁰, Asia Ahmed⁸⁰, Magali N. Taylor⁸⁰, Arjun Nair^{80,81}, David Lawrence⁸², Davide Patrini⁸², Neal Navani^{83,84}, Ricky M. Thakrar^{83,84}, Sam M. Janes⁸⁵, Emilie Martinoni Hoogenboom⁷¹, Fleur Monk⁷¹, James W. Holding⁷¹, Junaid Choudhary⁷¹, Kunal Bhakri⁷¹, Marco Scarci⁷¹, Pat Gorman⁷¹, Reena Khuroy⁷, Robert CM Stephens⁷¹, Yien Ning Sophia Wong⁷¹, Zoltan Kaplar^{86,87}, Steve Bandula⁷¹, Anne-Marie Hacker¹⁰, Abigail Sharp¹⁰, Sean Smith¹⁰, Harjot Kaur Dhanda¹⁰, Camilla Pilotti¹⁰, Rachel Leslie¹⁰, Anca Grapa⁸⁸, Hanyun Zhang⁸⁸, Khalid AbdulJabbar⁸⁹, Xiaoxi Pan⁹⁰, Yinyin Yuan⁹⁰, David Chuter⁹¹, Mairead MacKenzie⁹¹, Serena Chee⁹², Aiman Alzetani⁹², Judith Cave⁹³, Jennifer Richards⁹², Eric Lim^{94,95}, Paulo De Sousa⁹⁵, Simon Jordan⁹⁵, Alexandra Rice⁹⁵, Hilgardt Raubenheimer⁹⁵, Harshil Bhayani⁹⁵, Lyn Ambrose⁹⁵, Anand Devaraj⁹⁵, Hema Chavan⁹⁵, Sofina Begum⁹⁵, Silviu I. Buder⁹⁵, Daniel Kaniu⁹⁵, Mpho Malima⁹⁵, Sarah Booth⁹⁵, Andrew G. Nicholson^{95,96}, Nadia Fernandes⁹⁵, Pratibha Shah⁹⁵, Chiara Proli⁹⁵, Madeleine Hewish^{97,98}, Sarah Danson^{99,100}, Michael J. Shackcloth¹⁰¹, Lily Robinson¹⁰², Peter Russell¹⁰², Kevin G. Blyth^{103,104,105}, Andrew Kidd¹⁰⁶, Craig Dick¹⁰⁷, John Le Quesne^{108,109,110}, Alan Kirk¹¹¹, Mo Asif¹¹¹, Rocco Bilancia¹¹¹, Nikos Kostoulas¹¹¹ & Mathew Thomas¹¹¹

¹²Singleton Hospital, Swansea Bay University Health Board, Swansea, UK. ¹³University Hospitals of Leicester NHS Trust, Leicester, UK. ¹⁴Leicester Medical School, University of Leicester, Leicester, UK. ¹⁵University of Leicester, Leicester, UK. ¹⁶Cancer Research Centre, University of Leicester, Leicester, UK. ¹⁷Royal Free London NHS Foundation Trust, London, UK. ¹⁸Aberdeen Royal Infirmary NHS Grampian, Aberdeen, UK. ¹⁹Department of Medical Oncology, Aberdeen Royal Infirmary NHS Grampian, Aberdeen, UK. ²⁰University of Aberdeen, Aberdeen, UK. ²¹Department of Pathology, Aberdeen Royal Infirmary NHS Grampian, Aberdeen, UK. ²²The Whittington Hospital NHS Trust, London, UK. ²³Birmingham Acute Care Research Group, Institute of Inflammation and Ageing, University of Birmingham, Birmingham, UK. ²⁴Guy's and St Thomas' NHS Foundation Trust, London, UK. ²⁵University Hospital Birmingham NHS Foundation Trust, Birmingham, UK. ²⁶Institute of Immunology and Immunotherapy, University of Birmingham, Birmingham, UK. ²⁷Manchester Cancer Research Centre Biobank, Manchester, UK. ²⁸Wythenshawe Hospital, Manchester University NHS Foundation Trust, Wythenshawe, UK. ²⁹Manchester University NHS Foundation Trust, Manchester, UK. ³⁰Division of Infection, Immunity and Respiratory Medicine, University of Manchester, Manchester, UK. ³¹Cancer Research UK Lung Cancer Centre of Excellence, University of Manchester, Manchester, UK. ³²The Christie NHS Foundation Trust, Manchester, UK. ³³Division of Cancer Sciences, The University of Manchester and The Christie NHS Foundation Trust, Manchester, UK. ³⁴Cancer Research UK Manchester Institute Cancer Biomarker Centre, University of Manchester, Manchester, UK. ³⁵Artificial Intelligence in Medicine (AIM) Program, Mass General Brigham, Harvard Medical School, Boston, MA, USA. ³⁶Department of Radiation Oncology, Brigham and Women's Hospital, Dana-Farber Cancer Institute, Harvard Medical School, Boston, MA, USA. ³⁷Radiology and Nuclear Medicine, CARIM & GROW, Maastricht University, Maastricht, The Netherlands. ³⁸Institute for Computational Cancer Biology, Center for Integrated Oncology (CIO), Cancer Research Center Cologne Essen (CCCE), Faculty of Medicine and University Hospital Cologne, University of Cologne, Cologne, Germany. ³⁹Berlin Institute for the Foundations of Learning and Data (BIFOLD), Berlin, Germany. ⁴⁰Berlin Institute for Medical Systems Biology, Max Delbrück Center for Molecular Medicine in the Helmholtz Association (MDC), Berlin, Germany. ⁴¹Department of Genetics, The University of Texas MD Anderson Cancer Center, Houston, Texas, USA. ⁴²Department of Genomic Medicine, The University of Texas MD Anderson Cancer Center, Houston, Texas, USA. ⁴³Cancer Genomics Laboratory, The Francis Crick Institute, London, UK. ⁴⁴Department of Molecular Medicine, Aarhus University Hospital, Aarhus, Denmark. ⁴⁵Department of Clinical Medicine, Aarhus University, Aarhus, Denmark. ⁴⁶Bioinformatics Research Centre, Aarhus University, Aarhus, Denmark. ⁴⁷Danish Cancer Society Research Center, Copenhagen, Denmark. ⁴⁸Computational Health Informatics Program, Boston Children's Hospital, Boston, MA, USA. ⁴⁹Department of Bioinformatics, Semmelweis University, Budapest, Hungary. ⁵⁰Department of Pathology, ZAS Hospitals, Antwerp, Belgium. ⁵¹Division of Research, Peter MacCallum Cancer Centre, Melbourne, Australia. ⁵²Department of Physics of Complex Systems, ELTE Eötvös Loránd University, Budapest, Hungary. ⁵³Integrative Cancer Genomics Laboratory, VIB Center for Cancer Biology, Leuven, Belgium. ⁵⁴VIB Center for AI & Computational Biology, Leuven, Belgium. ⁵⁵Department of Oncology, KU Leuven, Leuven, Belgium. ⁵⁶Computational Cancer Genomics Research Group, University College London Cancer Institute, London, UK. ⁵⁷University College London Cancer Institute, London, UK. ⁵⁸The Francis Crick Institute, London, UK. ⁵⁹Medical Genomics, University College London Cancer Institute, London, UK. ⁶⁰Bill Lyons Informatics Centre, University College London Cancer Institute, London, UK. ⁶¹Experimental Histopathology, The Francis Crick Institute, London, UK. ⁶²Department of Infectious Disease, Faculty of Medicine, Imperial College London, London, UK. ⁶³Advanced Sequencing Facility, The Francis Crick Institute, London, UK. ⁶⁴Department of Haematology, University College London Hospitals, London, UK. ⁶⁵Cancer Immunology Unit, Research Department of Haematology, University College London Cancer Institute, London, UK. ⁶⁶Tumour Immunogenomics and Immunosurveillance Laboratory, University College London Cancer Institute, London, UK. ⁶⁷Retroviral Immunology Group, The Francis Crick Institute, London, UK. ⁶⁸Bioinformatics and Systems Biology, Method Development and Research Infrastructure, Robert Koch Institute, Berlin, Germany. ⁶⁹Experimental Oncology, Institute for Oncology and Radiology of Serbia, Belgrade, Serbia. ⁷⁰University College London Department of Epidemiology and Health Care, London, UK. ⁷¹University College London Hospitals, London, UK. ⁷²Department I of Internal Medicine, University Hospital of Cologne, Cologne, Germany. ⁷³Immune Regulation and Tumour Immunotherapy Group, Cancer Immunology Unit, Research Department of Haematology, University College London Cancer Institute, London, UK. ⁷⁴Cancer Evolution and Genome Instability Laboratory, The Francis Crick Institute, London, UK. ⁷⁵Centre for Medical Image Computing, Department of Medical Physics and Biomedical Engineering, University College London, London, UK. ⁷⁶Department of Medical Physics and Bioengineering, University College London Cancer Institute, London, UK. ⁷⁷Department of Medical Physics and Biomedical Engineering, University College London, London, UK. ⁷⁸Institute of Nuclear Medicine, Division of Medicine, University College London, London, UK. ⁷⁹Institute of Structural and Molecular Biology, University College London, London, UK. ⁸⁰Department of Radiology, University College London Hospitals, London, UK. ⁸¹UCL Respiratory, Department of Medicine, University College London, London, UK. ⁸²Department of Thoracic Surgery, University College London Hospital NHS Trust, London, UK. ⁸³Lungs for Living Research Centre, UCL Respiratory, University College London, London, UK. ⁸⁴Department of Thoracic Medicine, University College London Hospitals, London, UK. ⁸⁵Lungs for Living Research Centre, UCL Respiratory, Department of Medicine, University College London, London, UK. ⁸⁶Integrated Radiology Department, North-buda St. John's Central Hospital, Budapest, Hungary. ⁸⁷Institute of Nuclear Medicine, University College London Hospitals, London, UK. ⁸⁸The Institute of Cancer Research, London, UK. ⁸⁹Case45, London, UK. ⁹⁰The University of Texas MD Anderson Cancer Center, Houston, USA. ⁹¹Independent Cancer Patients' Voice, London, UK. ⁹²University Hospital Southampton NHS Foundation Trust, Southampton, UK. ⁹³Department of Oncology, University Hospital Southampton NHS Foundation Trust, Southampton, UK. ⁹⁴Academic Division of Thoracic Surgery, Imperial College London, London, UK. ⁹⁵Royal Brompton and Harefield Hospitals, part of Guy's and St Thomas' NHS Foundation Trust, London, UK. ⁹⁶National Heart and Lung Institute, Imperial College, London, UK. ⁹⁷Royal Surrey Hospital, Royal Surrey Hospitals NHS Foundation Trust, Guildford, UK. ⁹⁸University of Surrey, Guildford, UK. ⁹⁹University of Sheffield, Sheffield, UK. ¹⁰⁰Sheffield Teaching Hospitals NHS Foundation Trust, Sheffield, UK. ¹⁰¹Liverpool Heart and Chest Hospital, Liverpool, UK. ¹⁰²Princess Alexandra Hospital, The Princess Alexandra Hospital NHS Trust, Harlow, UK. ¹⁰³School of Cancer Sciences, University of Glasgow, Glasgow, UK. ¹⁰⁴Beatson Institute for Cancer Research, University of Glasgow, Glasgow, UK. ¹⁰⁵Queen Elizabeth University Hospital, Glasgow, UK. ¹⁰⁶Institute of Infection, Immunity & Inflammation, University of Glasgow, Glasgow, UK. ¹⁰⁷NHS Greater Glasgow and Clyde, Glasgow, UK. ¹⁰⁸Cancer Research UK Scotland Institute, Glasgow, UK. ¹⁰⁹Institute of Cancer Sciences, University of Glasgow, Glasgow, UK. ¹¹⁰NHS Greater Glasgow and Clyde Pathology Department, Queen Elizabeth University Hospital, Glasgow, UK. ¹¹¹Golden Jubilee National Hospital, Clydebank, UK.

Methods

Baseline characterization of lung cancer samples

TRACERx patient recruitment and sample collection complied with all relevant ethical regulations and were carried out as previously described². The eligibility criteria have been previously described². Of note, the eighth version of pTNM staging was used in this analysis. Patients with histopathologically confirmed stage I–IIIB NSCLC who were eligible for primary surgery were enrolled in the prospective observational TRACERx study (ClinicalTrials.gov identifier: [NCT01888601](https://clinicaltrials.gov/ct2/show/study/NCT01888601)). The study design was approved by an independent research ethics committee (NRES Committee London, REC ref. 13/LO/1546), and informed consent was obtained from all patients before study admittance. Patient sample identifiers were anonymized and tracked in a centralized database controlled by the study sponsor. DNA degradation of archived formalin-fixed paraffin-embedded (FFPE) samples over time can affect panel quality for ctDNA detection, and degraded samples might not accurately reflect the typical sample quality in a clinical setting in which FFPE samples were recently collected (Extended Data Fig. 4a). We obtained FFPE tissue for 204 patients. Of these, 62 had atypically low counts of high-quality panel targets (<1,000), likely owing to age and/or poor quality of the FFPE samples, and 2 did not pass panel design. For 31 of the 64 patients, DNA extracted from fresh frozen (FF) tissue was available by September 2023. For these samples, an updated set of panels was generated, the quality of which was more consistent with <5-year-old FFPE samples (Extended Data Fig. 4b). One panel was constructed from an FF tumor sample and failed to attain 1,000 high-quality targets; however, this was included to ensure that the cohort was representative of the wider TRACERx cohort. Two FF panels were constructed where FFPE panel construction had failed entirely. The final cohort in our study consisted of preoperative samples from 171 consecutively recruited patients in the larger TRACERx study in whom adequate plasma was available for the ctDNA analysis completed by September 2023, in addition to confirmed clinical outcome data as of February 2024. Retrospective ctDNA analysis was conducted using prospectively collected specimens and during clinical follow-up. In this cohort, we demonstrated that our measure of ctDNA signal (ppm) was in strong agreement with tumor molecules per ml plasma, which accounts for the volume of plasma from which input cfDNA is extracted (Demming regression; fitted slope = 0.97, CI = 0.95–0.99; Extended Data Fig. 4c). Personalis investigators were fully blinded to patient clinical outcome and clinical pathological characteristics during sample processing and ctDNA analysis. Likewise, TRACERx investigators were blinded to patient ctDNA status during clinical data and patient specimen collection. *EGFR* mutations, oncogenic fusion isoforms and instances of *MET* exon 14 skipping from patients in the TRACERx cohort were annotated as previously described²⁹.

Tumor and normal whole-genome sequencing

Tumor sections were macrodissected to improve tumor content and were required to meet a tumor cellularity threshold of $\geq 20\%$, as determined by pathological review, to be eligible for DNA extraction and further processing. At this threshold, 1.2% (2/171) of samples were considered ineligible for analysis and required replacement with different specimens. At our chosen 20% cut-off threshold, we observed no significant correlation between tumor purity and the LOD of the assay (Supplementary Fig. 1). Genomic DNA was isolated from matched tumor and normal samples using the Qiagen AllPrep DNA/RNA FFPE Tissue Kit or the QIAamp DNA Mini Kit (Qiagen) using internally optimized workflows. Whole-genome sequencing (WGS) libraries were prepared with 100–500 ng of acoustically sheared genomic DNA (Covaris) using the KAPA HyperPrep Kit (Roche Sequencing Solutions) and customized methods. Libraries were cleaned up using AMPure XP beads and then quantified using the KAPA Library Quantification Kit (Roche Sequencing Solutions), before being sequenced to $\times 30$ depth of coverage using a NovaSeq 6000 instrument (Illumina). The impact

of varying DNA input amounts during tumor WGS on panel design was assessed using 19 normal–tumor pairs. For each pair, normal libraries were made using 550 ng input DNA, and tumor libraries with 5 ng, 15 ng, 50 ng, 200 ng or 550 ng of input DNA. We observed largely consistent panel size and similarity across the range of input DNA amounts (Supplementary Fig. 2a,b). A comprehensive list of reagents used in this study is provided in Supplementary Table 1.

Alignment and variant calling from tumor and normal whole-genome sequencing

The pipeline performs alignment, duplicate removal and base quality-score recalibration (BQSR) of the matched tumor and normal WGS samples using best-practice guidelines recommended by the Broad Institute^{30,31}. In brief, individual read-pairs were first mapped to the hs37d5 reference genome build using the BWA–MEM aligner. We then used the Picard toolkit (RRID: [SCR_006525](https://www.ncbi.nlm.nih.gov/RRID/SCR_006525)) to identify duplicate reads through comparison of the 5' position of reads and read-pairs. Duplicate reads were then removed. The Genome Analysis Toolkit (GATK, RRID: [SCR_001876](https://www.ncbi.nlm.nih.gov/RRID/SCR_001876)) was then used for sequence realignment and to apply base quality scores (BQSR): the BaseRecalibrator tool uses the deduplicated data and a set of known variants to construct a model of covariation, which is used to generate a recalibration file. The ApplyBQSR tool then uses this model to adjust base quality scores in the data, yielding a new BAM file. Aligned sequence data are written in BAM format according to SAM (RRID: [SCR_01095](https://www.ncbi.nlm.nih.gov/RRID/SCR_01095)) specification. MuTect (RRID: [SCR_000559](https://www.ncbi.nlm.nih.gov/RRID/SCR_000559)) was used to co-analyze the tumor and normal BAM files for somatic single-nucleotide variant (SNV) detection. Somatic SNV calls were filtered on the basis of a broad set of quality-control metrics, such as local sequence coverage and read quality, strand bias and the statistical likelihood that the allele is present in the normal sample.

NeXT personal probe panel design

Hybrid capture probe panels used in this study were designed with the NeXT Personal platform's proprietary algorithms, as governed by the standard operating procedures at Personalis. In the design process for the bespoke panel, for each patient's panel, the ctDNA targets were selected from exonic, intronic and intergenic somatic variants identified through WGS of matched tumor and normal samples, as described above. Somatic variants identified using Mutect (v1.1.6, default parameters) were selected and assigned an error rate according to the observed substitution in the solid tumor. Namely, the substitution error rate was estimated by the ratio of the aggregated amount of signal and the total number of molecules observed in each possible substitution in more than 200 healthy plasma samples²³. The MRD targets were then selected from somatic variants with an allele frequency above 10%. Variants were further filtered by excluding those found in particular regions of the genome. Exclusion criteria included regions containing known germline SNPs, known CHIP variants, high GC content ($\geq 80\%$), high polymorphism rates, mapping difficulties, systematic bias, short tandem repeats and low sequence complexity³².

Somatic variant calls were ranked by the product of allele frequency in solid tumor and the substitution-based error rate of solid tumor substitutions. Up to $\sim 1,800$ top ranked somatic variants were selected genome-wide for panel inclusion by the NeXT Personal platform. The final panel also included 43 population SNVs for quality-assurance purposes (that is, to detect potential sample–panel mismatch or contamination). Several criteria were used to optimize the selection of the 43 SNVs, including having a population frequency of at least 20%, being in Hardy–Weinberg equilibrium and being outside of the HLA region. The SNPs were prioritized to have roughly equivalent representation across subpopulations. Probe sequences were designed by the NeXT Personal platform's proprietary algorithm before being processed for manufacturing. Upon receiving panel reagents, the new panel was used for targeted sequencing of blood

plasma from an unrelated healthy donor. This served two purposes: quality-control tests on the sequencing data were used to qualify the panel for use on the patient's plasma samples, and any MRD targets for which any non-reference signal was observed were deactivated in the logical panel design, to mitigate the risk that those targets could be enriched for noise.

NeXT Personal cfDNA library preparation, target enrichment and sequencing

Library preparation, target enrichment and sequencing of the cfDNA samples were performed in CLIA-certified and CAP-accredited laboratories, as governed by the standard operating procedures at Personalis. In brief, sequencing libraries were prepared from 2.45–50 ng cfDNA input (median, 15 ng), using the KAPA HyperPrep Kit (Roche Sequencing Solutions) and customized methods. We assessed the effect of the quantity of total input cfDNA on MRD detection and ctDNA burden and observed no significant associations between the amount of cfDNA input and ctDNA detection status (Supplementary Fig. 3). Consistently, there was no significant correlation between the quantity of input cfDNA and ctDNA burden or ctDNA burden and the LOD of the assay (Supplementary Fig. 3b,c). Together, this evidence suggests that ctDNA burden and detection status were not confounded by the quantity of total circulating DNA in the cohort. These findings are supported by a separate analytical validation study²³. The pre-capture libraries were quantified using a Lunatic spectrophotometer (Unchained Labs), and up to 1,500 ng was enriched with patient-specific NeXT Personal probe panels using proprietary modifications to the Fast Hybridization and Wash Kit (Twist Bioscience) and workflow. The postcapture libraries were then amplified by PCR (nine cycles), and a quality assessment was performed using the TapeStation system (Agilent Technologies). The final libraries were cleaned up using AMPure XP beads and then quantified using the KAPA Library Quantification Kit (Roche Sequencing Solutions) before being sequenced on a NovaSeq 6000 instrument (Illumina). The libraries were deeply sequenced to optimize the number of unique observed molecules. We observed a weak correlation between sequencing depth and the LOD for each custom assay, as well as between sequencing depth and the strength of ctDNA signal detected (ppm level); however, the ctDNA detection status (detected or not detected) was not confounded by the variability of sequencing depth, with no significant difference in sequencing depth observed between the two groups (Supplementary Fig. 4a–c).

NeXT Personal cfDNA analysis

Analysis of all NeXT Personal data in this study was performed using a consistent, locked version of the production pipeline developed by Personalis. In summary, the cfDNA sequencing data were aligned to the human reference genome (version hs37d5), followed by noise suppression and ctDNA detection. More specifically, we built and filtered the molecular consensus as follows. First, we aligned all reads to the human reference using BWA–MEM (Burrows–Wheeler Aligner, v1.0.2). Second, we grouped read-pairs according to their paired mapped positions to form initial consensus groups. With a positional approach like this, there is a risk of grouping multiple molecules together that share paired mapped positions. We mitigated this risk by detecting the presence of non-reference alleles that were present in not only a subset of the consensus-group reads, but also at least two other consensus groups. When there was an allele present in a subset of reads with additional support from other consensus groups, we split the consensus group to isolate the allele-containing reads in their own new group. For each group, we required observation of at least one molecule from each DNA strand. Raw reads that differed by more than 2.5% across the consensus molecule were not included. Bases with a quality of less than 29 were masked. Once we defined the consensus groups, we formed a single consensus molecule from the reads in each group on the basis of identification of the consensus basecall at

each position along the group of read-pairs. Bases with less than 90% agreement in the molecular group were masked. Reads with more than 20% of their bases masked were removed. Then, we re-mapped these consensus reads again using BWA–MEM to avoid any erroneous alignment caused by sequencing errors. Following noise suppression, tumor-derived signal was aggregated in a tested sample across ctDNA targets in each patient-specific panel to calculate the ctDNA level (measured in ppm, based on the total unique molecule count). A one-tailed Poisson test was then performed to determine ctDNA detection status for each tested sample. The observed aggregate tumor-derived signal across each panel serves as the tested value, with the expected noise arising from accumulated background error being set as the mean of the Poisson distribution. The *P* value threshold was established as previously described²³. In brief, the *P* value threshold is set at <0.001 to ensure that an analytical specificity requirement of >99.9% was met. Therefore, the *P* value threshold was set to 0.001 for this study to ensure higher specificity. If the tumor signal was significantly ($P \leq 0.001$) above the expected noise, the sample was classified as ctDNA-positive (that is 'detected'); otherwise, it was classified as ctDNA-negative (that is 'not detected'). Given that the *P* value is the probability that the observed signal comes from noise, the detection threshold is set to enforce a specificity requirement and is independent of factors that affect observed levels. Variations in assay and locus-specific factors might affect the efficiency of detection of a specific genetic alteration. Different genetic alterations could also be present at different frequencies in the blood. The actual ppm level (allele frequency) measured is a function of the set of targets selected. After aggregation across many loci, however, the average per-locus efficiency of detection tends toward the population mean of the efficiency of detecting a specific genetic alteration. This is demonstrated in Supplementary Figure 5a, which shows that, as the panel size approaches 1,800 targets, the coefficient of variation (CV) of the observed ppm level adds little to the overall variability of the assay. Basing detection status on a *P* value, rather than an allele frequency threshold, allowed our approach to normalize detection efficiency for specific mutations through the summation of signal across up to 1,800 variant loci that have been selected on the basis of their site-specific error rates, inherent noise and complexity.

Clonal hematopoiesis of indeterminate potential

We designed our assay to prevent CHIP mutations from being included in the bespoke panel by taking a tumor-matched-normal approach for somatic variant calling to inform panel design. This is an effective approach because the CHIP signal is higher in the normal blood cells than in tumor tissue, and thus will be filtered out in the tumor normal algorithmic comparison. We also excluded the most common CHIP regions from our panel design.

TRACERx cfDNA extraction and quantification

Blood samples were collected in K₂-EDTA tubes. Samples were processed within 2 h of collection by double centrifugation of the blood, first for 10 min at 1,000g, then the plasma for 10 min at 2,000g. Plasma was stored in 1-ml aliquots at –80 °C. Following isolation, plasma was shipped on dry ice. At the time of analysis, TRACERx plasma samples were between 2 and 9 years old. Up to 24 h before cfDNA extraction, the plasma was thawed and aliquots from the same patient plasma time point were consolidated and then stored at 4 °C. Immediately before cfDNA extraction using QIAamp Circulating Nucleic Acid or QIASymphony Circulating DNA kits (Qiagen), consolidated plasma was clarified at 16,000g to remove cryoprecipitates.

Samples used for DNA input performance characterization

All experiments were performed in the Clinical Laboratory Improvement Amendments (CLIA)-certified and College of American Pathologists (CAP)-accredited laboratories at Personalis, as guided by the

Association for Molecular Pathology (AMP) and CAP's joint recommendations³³. Healthy donor and patient tissue and matched buffy-coat and plasma samples used in Supplementary Figures 2 and 5 were sourced from either Boca Biolistics, Cureline or iProcess. Patient samples in this study obtained from commercial vendors were collected from informed patients following receipt of their written consent under study protocols approved by an Independent Ethical Committee or Institutional Review Board (Protocol numbers: PG-ONC 2003/1; IRB7 -Registration 5136; IRB 800959).

Survival analyses

OS was defined as the days from registration to death or loss of follow-up. RFS was defined as the days from registration to any disease recurrence, new primary tumor events or death. Exploratory analysis comparing OS and RFS at different ctDNA levels was performed for a total 171 patients shown in Figure 2 and Extended Data Figure 3. Survival (3.3–1), survminer (0.4.9) and finalfit (1.0.4) R packages were used to generate hazard ratios, CIs, 2-year survival probability, forest plots, KM plots and Cox regression models. Differences in OS or RFS between different groups of patients were assessed using log-rank tests. The association of OS or RFS with continuous variables, such as ctDNA level, was assessed through Cox regression modeling. The independent prognostic value of ctDNA in either the continuous or categorical form was assessed by multivariable Cox regression models that included histology, adjuvant treatment status, smoking status, pathological stage and age.

Statistical analysis and data handling

No statistical methods were used to predetermine sample size. Analysis was performed in the R statistical environment (4.1.3). All statistical tests were two-sided, unless stated otherwise. For assay-performance analyses, positive predictive value was calculated as all true-positive results divided by the sum of true-positive and false-positive results; negative predictive value was calculated as all true-negative results divided by the sum of false-negative plus true-negative results; sensitivity was calculated as true-positive results divided by the sum of true-positive and false-negative results; and specificity was calculated as true negatives divided by the sum of true negatives and false positives. For input and output operations and general data manipulation, the R packages tidyverse (v1.3.2) and lubridate were used (v1.9.2). For general visualization, the R packages ggplot2 (v.3.4.2), ggpubr (v.0.4.0), scales (v.1.2.1) and ggnewscale (v.0.4.9) were used. For statistical analyses and related visualization, R packages survival (v.3.3–1), survminer (v.0.4.9), finalfit (v.1.0.4), gt (v.0.10.1) and mcr (v.1.2.2) were used.

Reporting summary

Further information on research design is available in the Nature Portfolio Reporting Summary linked to this article.

Data availability

Processed TRACERx patient data have been deposited on Zenodo at <https://doi.org/10.5281/zenodo.8400837> (ref. 34). Supporting data from validation experiments are included as Extended Data Table 1. Raw data from TRACERx patients analyzed in this study, including fastq and bam files from tumor and normal WGS, as well as fastq files from cfDNA, have been deposited at the European Genome-phenome Archive (EGA), hosted by The European Bioinformatics Institute (EBI) and the Centre for Genomic Regulation (CRG) under the accession codes [EGAS00001006494](https://doi.org/10.5555/EGAS00001006494), under controlled access.

Code availability

Supporting code required to reproduce all analyses and figures included in this paper are available on Zenodo at <https://doi.org/10.5281/zenodo.8400837> (ref. 34).

References

- Frankell, A. M. et al. The evolution of lung cancer and impact of subclonal selection in TRACERx. *Nature* **616**, 525–533 (2023).
- Van der Auwera, G. A. & O'Connor, B. D. *Genomics in the Cloud: Using Docker, GATK, and WDL in Terra* (O'Reilly Media, 2020).
- DePristo, M. A. et al. A framework for variation discovery and genotyping using next-generation DNA sequencing data. *Nat. Genet.* **43**, 491–498 (2011).
- Freeman, T. M. et al. Genomic loci susceptible to systematic sequencing bias in clinical whole genomes. *Genome Res.* **30**, 415–426 (2020).
- Jennings, L. J. et al. Guidelines for validation of next-generation sequencing-based oncology panels: a joint consensus recommendation of the Association for Molecular Pathology and College of American Pathologists. *J. Mol. Diagn.* **19**, 341–365 (2017).
- Black, J. An ultra-sensitive and specific ctDNA assay provides novel pre-operative disease stratification in early stage lung adenocarcinoma. Zenodo <https://doi.org/10.5281/zenodo.8400837> (2024).

Acknowledgements

We thank the staff of the Advanced Sequencing Facility at The Francis Crick Institute, as well as the members of the TRACERx consortium for their contributions to this study. TRACERx (ClinicalTrials.gov no.: NCT01888601) is sponsored by University College London (UCL/12/O279) and was approved by an independent research ethics committee (REC 13/LO/1546). TRACERx is funded by Cancer Research UK (CRUK; C11496/A17786) and is coordinated by CRUK and the UCL Cancer Trials Centre, which has a core grant from CRUK (C444/A15953). We gratefully acknowledge the patients and relatives who participated in the TRACERx study; all site personnel, investigators, funders and industry partners that supported the generation of the data within this study. This work was also supported by the CRUK Lung Cancer Centre of Excellence and the CRUK City of London Centre Award (C7893/A26233) as well as the UCL Experimental Cancer Medicine Centre. We acknowledge the Personalis research and development team for their work in developing and validating the NeXT Personal platform, including major contributions from J. Li and A. Stram. We also acknowledge the Personalis operations team for helping to process the samples using NeXT Personal. T.K. is supported by the Japan Society for the Promotion of Science (JSPS) overseas research fellowships program (202060447). M.J.-H. is a CRUK Fellow and has received funding from CRUK, NIHR, the Rosetrees Trust, UKI NETs and the NIHR University College London Hospitals Biomedical Research Centre. N.M. is a Sir Henry Dale Fellow, jointly funded by the Wellcome Trust and the Royal Society (211179/Z/18/Z), and also receives funding from CRUK, the Rosetrees Trust, the NIHR BRC at University College London Hospitals and the CRUK University College London Experimental Cancer Medicine Centre. C.S. is a Royal Society Napier Research Professor (RSRP\R\210001). His work is supported by the Francis Crick Institute, which receives its core funding from Cancer Research UK (CC2041), the UK Medical Research Council (CC2041) and the Wellcome Trust (CC2041). For the purpose of Open Access, the author has applied a CC BY public copyright licence to any author accepted manuscript version arising from this submission. C.S. is funded by Cancer Research UK (TRACERx (C11496/A17786), PEACE (C416/A21999) and CRUK Cancer Immunotherapy Catalyst Network); Cancer Research UK Lung Cancer Centre of Excellence (C11496/A30025); the Rosetrees Trust, Butterfield and Stonegate Trusts; NovoNordisk Foundation (ID16584); Royal Society Professorship Enhancement Award (RP/EA/180007 and RF\ERE\231118); National Institute for Health Research (NIHR) University College London Hospitals Biomedical Research Centre; the Cancer Research UK-University College London Centre; Experimental Cancer Medicine

Centre; the Breast Cancer Research Foundation (US) (BCRF-22-157); Cancer Research UK Early Detection and Diagnosis Primer Award (Grant EDDPMA-Nov21/100034); and The Mark Foundation for Cancer Research Aspire Award (Grant 21-029-ASP) and ASPIRE Phase II award (Grant 23-034-ASP). C.S. received an ERC Advanced Grant (PROTEUS) from the European Research Council under the European Union's Horizon 2020 research and innovation program (grant agreement no. 835297).

Author contributions

J.R.M.B. and C.S. designed the clinical portion of the study. S.V. and M.C. coordinated handling of clinical specimens. J.R.M.B., M.S.H., K.T., A.H., C.B., E.C.C., C.M.R., K.G. and P.P. performed quality control of genomic data. T.K., M.A.B., W.K.L., D.A.M., D.M., O.G.S., C.M., M.S. and J.R.M.B. performed quality control on clinical data. M.A.B., D.A.M., J.A.S., A.H., M.J.-H. and C.S. coordinated the TRACERx clinical trial. R.O.C. and G.B. conceived the NeXT Personal platform. G.B. created the panel design and ctDNA-detection algorithms. G.B., R.M.P. and F.C.P.N. developed the noise-suppression methods. J.L., J.N. and G.B. designed the analytical study and analyzed the associated data. J.N. and J.L. led the assay development and analytical study experiments. J.H. led the pipeline development. Clinical data were analyzed by J.R.M.B., and then analyzed separately by C.W.A. and B.L. J.R.M.B., A.M.F., N.M., C.W.A., R.O.C., J.L., G.B., J.H., R.C., J.N., R.P., S.B. and C.S. prepared the manuscript. R.O.C. and C.S. jointly supervised the study.

Funding

Open Access funding provided by The Francis Crick Institute.

Competing interests

M.A.B. has consulted for Achilles Therapeutics. D.A.M. reports receiving speaker fees from AstraZeneca, Eli Lilly, Bristol Myers Squibb and Takeda, consultancy fees from AstraZeneca, Thermo Fisher, Takeda, Amgen, Janssen, MIM Software, Bristol Myers Squibb and Eli Lilly and has received educational support from Takeda and Amgen. M.J.-H. has consulted for, and is a member of, the Achilles Therapeutics scientific advisory board (SAB) and steering committee, and has received speaker honoraria from Pfizer, Astex Pharmaceuticals and the Oslo Cancer Cluster. N.M. has received consultancy fees and has stock options in Achilles Therapeutics. C.S. acknowledges grants from AstraZeneca, Boehringer-Ingelheim, Bristol Myers Squibb, Pfizer, Roche-Ventana, Invitae (previously Archer Dx Inc, collaboration in minimal residual disease sequencing technologies), Ono Pharmaceutical and Personalis. He is chief investigator for the AZ MeRmaid 1 and 2 clinical trials and is the steering committee chair. He is also co-chief investigator of the NHS Galleri trial funded by GRAIL and a paid member of GRAIL's SAB. He receives consultant fees from Achilles Therapeutics (and is a SAB member), Bicycle Therapeutics (and is a SAB member), Genentech, Medicxi, China Innovation Centre of Roche (formerly Roche Innovation Centre – Shanghai, Metabomed (until July 2022)), Relay Therapeutics (and is a SAB member), Saga Diagnostics (and is a SAB member) and the Sarah Cannon Research Institute. C.S. has received honoraria from Amgen, AstraZeneca, Bristol Myers Squibb, GSK,

illumina, MSD, Novartis, Pfizer and Roche-Ventana. C.S. has previously held stock options in Apogen Biotechnologies and GRAIL, and currently has stock options in Bicycle Therapeutics and Relay Therapeutics, and has stock and is a co-founder of Achilles Therapeutics. G.B., C.W.A., S.M.B., R.C., J.H., B.L., J.L., F.C.P.N., J.N., R.M.P. and R.O.C. are employees and stockholders of Personalis. A.M.F. is listed as a co-inventor on a patent application to determine methods and systems for tumor monitoring (PCT/EP2022/077987; 'Methods and systems for tumour monitoring'). S.V. is a co-inventor on a patent for methods for detecting molecules in a sample (US patent no. 10578620; 'Methods for detecting molecules in a sample'). M.J.-H. is listed as a co-inventor on a European patent application related to methods to detect lung cancer (PCT/US2017/028013; 'Methods for lung cancer detection'); this patent has been licensed to commercial entities and, under terms of employment, M.J.-H. is due a share of any revenue generated from such license(s). N.M. holds European patents related to targeting neoantigens (PCT/EP2016/059401; 'Method for treating cancer'), identifying patient response to immune checkpoint blockade (PCT/EP2016/071471; 'Immune checkpoint intervention in cancer'), determining HLA LOH (PCT/GB2018/052004; 'Analysis of HLA alleles in tumours and the uses thereof'), and predicting survival rates of patients with cancer (PCT/GB2020/050221; 'Method of predicting survival rates for cancer patients'). C.S. declares a patent application for methods to lung cancer (PCT/US2017/028013); targeting neoantigens (PCT/EP2016/059401); identifying patent response to immune checkpoint blockade (PCT/EP2016/071471); methods for lung cancer detection (US20190106751A1); identifying patients who respond to cancer treatment (PCT/GB2018/051912); determining HLA LOH (PCT/GB2018/052004); predicting survival rates of patients with cancer (PCT/GB2020/050221); and methods and systems for tumor monitoring (PCT/EP2022/077987). C.S. is an inventor on a European patent application (PCT/GB2017/053289) related to assay technology to detect tumor recurrence. This patent has been licensed to a commercial entity, and under their terms of employment, C.S. is due a revenue share of any revenue generated from such license(s). The other authors declare no competing interests.

Additional information

Extended data is available for this paper at <https://doi.org/10.1038/s41591-024-03216-y>.

Supplementary information The online version contains supplementary material available at <https://doi.org/10.1038/s41591-024-03216-y>.

Correspondence and requests for materials should be addressed to Charles Swanton.

Peer review information *Nature Medicine* thanks Alain Thierry, Benjamin Besse and the other, anonymous, reviewer(s) for their contribution to the peer review of this work. Primary Handling Editor: Anna Maria Ranzoni, in collaboration with the *Nature Medicine* team.

Reprints and permissions information is available at www.nature.com/reprints.

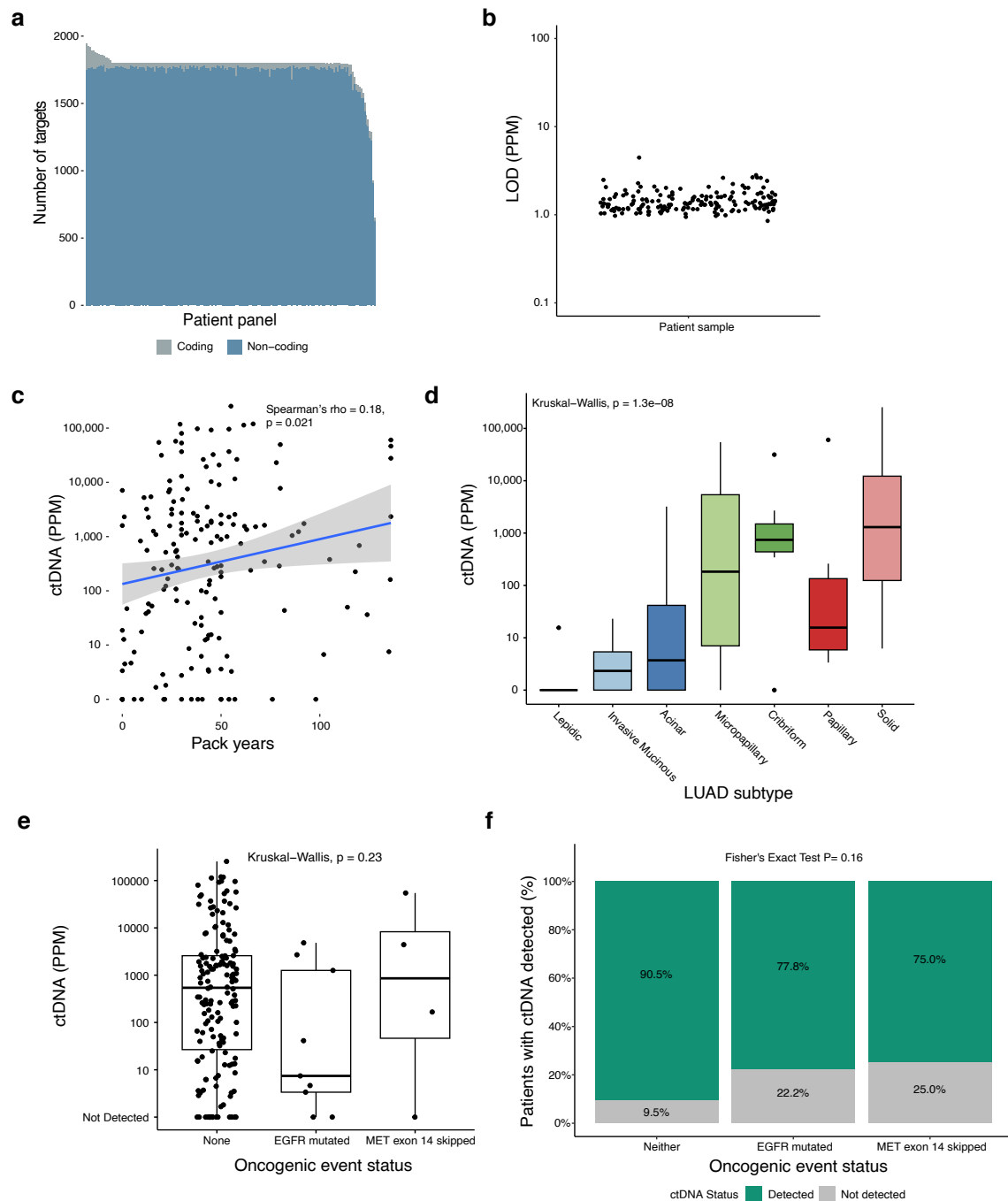
Extended Data Table 1 | Baseline demographic and tumor characteristics for the study population split by lung adenocarcinoma and non-adenocarcinoma populations. Data are *n* (%), unless otherwise stated. Percentages may not sum to 100% due to rounding

Characteristic	levels	LUAD	Non-LUAD	p
n	-	94	77	NA
Age (years)	Mean (SD)	67.2 (8.9)	70.1 (8.0)	0.028
Sex	Female	40 (42.6)	29 (37.7)	0.623
	Male	54 (57.4)	48 (62.3)	
Pathological TNM	1a	11 (11.7)	6 (7.8)	0.718
	1b	17 (18.1)	16 (20.8)	
	2a	4 (4.3)	4 (5.2)	
	2b	25 (26.6)	27 (35.1)	
	3a	35 (37.2)	22 (28.6)	
	3b	2 (2.1)	2 (2.6)	
Smoking status	Ex-Smoker	41 (43.6)	46 (59.7)	0.086
	Never Smoked	6 (6.4)	2 (2.6)	
	Smoker	47 (50.0)	29 (37.7)	
Adjuvant treatment	Adjuvant	46 (48.9)	36 (46.8)	0.896
	No adjuvant	48 (51.1)	41 (53.2)	
LUAD subtype	Lepidic	6 (6.4)		
	Papillary	6 (6.4)		
	Acinar	23 (24.5)		
	Cribriform	7 (7.4)		
	Micropapillary	4 (4.3)		
	Solid	38 (40.4)		
Oncogenic event	Invasive mucinous	10 (10.6)		0.364
	None	85 (90.4)	73 (94.8)	
	EGFR mutated	7 (7.4)	2 (2.6)	
	MET exon 14 skipped	2 (2.1)	2 (2.6)	
Follow up (days; OS)	Median (# of events)	1839 (39)	1862 (38)	0.84
Follow up (days; RFS)	Median (# of events)	1821 (49)	1849 (40)	0.58

P values were calculated using chi-squared tests for categorical variables and *t* tests for continuous variables.

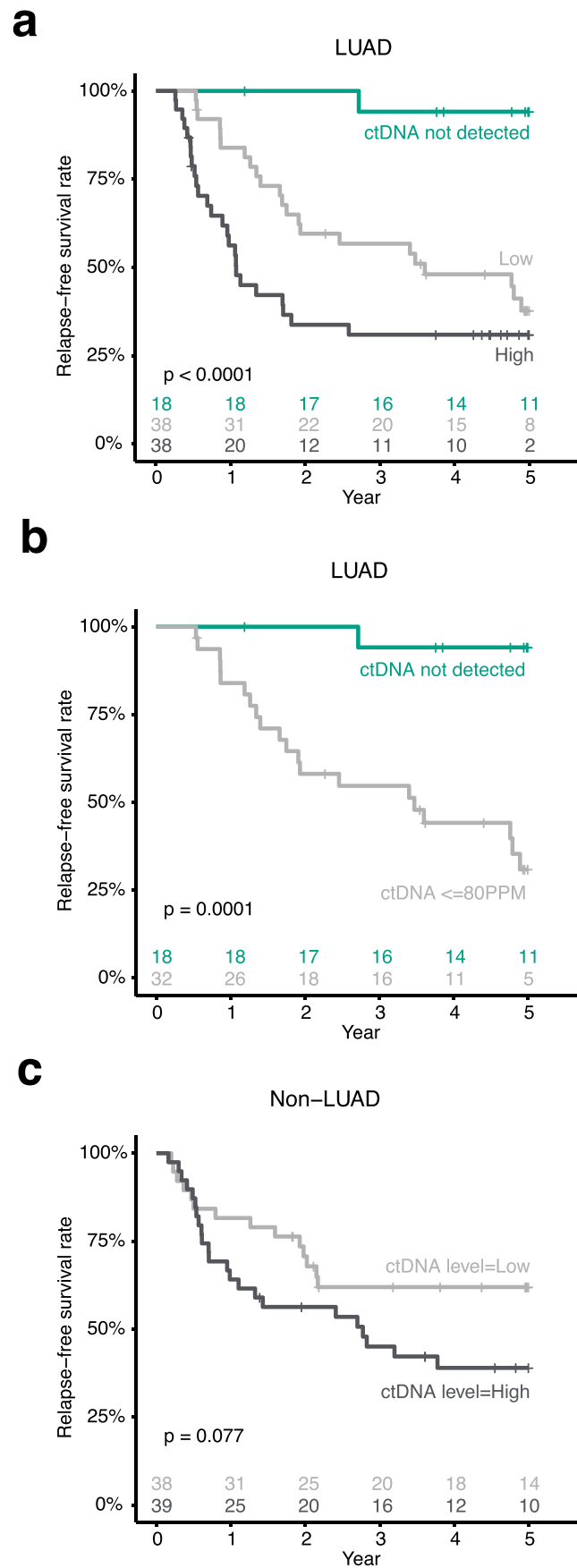
Extended Data Table 2 | Baseline demographic and tumor characteristics for the current study presented alongside general characteristics of patients included in the work detailed in refs. 1,2. Data are n (%), unless otherwise stated. Percentages may not sum to 100% due to rounding

Characteristic	levels	Abbosh et al. 2023	Abbosh et al. 2017	NeXT Personal
Age (years)	Mean (SD)	68.8 (9.4)	68.4 (9.3)	68.5 (8.6)
Sex	Female	79 (40.9)	36 (37.5)	69 (40.4)
	Male	114 (59.1)	60 (62.5)	102 (59.6)
Adjuvant treatment	Adjuvant	77 (39.9)	28 (29.2)	82 (48.0)
	No adjuvant	116 (60.1)	68 (70.8)	89 (52.0)
Histology	Adenocarcinoma	101 (52.3)	57 (59.4)	94 (55.0)
	Other	25 (13.0)	8 (8.3)	20 (11.7)
	Squamous cell carcinoma	67 (34.7)	31 (32.3)	57 (33.3)
LUAD subtype	Lepidic	4 (4.2)	10 (17.9)	6 (6.4)
	Papillary	11 (11.5)	4 (7.1)	6 (6.4)
	Acinar	33 (34.4)	21 (37.5)	23 (24.5)
	Cribiform	9 (9.4)	1 (1.8)	7 (7.4)
	Micropapillary	4 (4.2)		4 (4.3)
	Solid	24 (25.0)	14 (25.0)	38 (40.4)
	Invasive Mucinous	11 (11.5)	6 (10.7)	10 (10.6)
Pathological TNM	IA	37 (19.2)	26 (27.1)	17 (9.9)
	IB	37 (19.2)	32 (33.3)	33 (19.3)
	IIA	40 (20.7)	14 (14.6)	8 (4.7)
	IIB	30 (15.5)	10 (10.4)	52 (30.4)
	IIIA	49 (25.4)	13 (13.5)	57 (33.3)
	IIIB		1 (1.0)	4 (2.3)
Smoking status	Ex-Smoker	103 (53.4)	49 (51.0)	87 (50.9)
	Never Smoked	10 (5.2)	11 (11.5)	8 (4.7)
	Smoker	80 (41.5)	36 (37.5)	76 (44.4)



Extended Data Fig. 1 | Association between ctDNA and clinicogenomic features of NSCLC. a. Stacked barplot of the number of targets obtained from coding (grey) and noncoding (blue) regions of the genome for each panel. **b.** Dot plot depicting panel-specific limit of detection (LOD) in ppm in all pre-operative plasma samples. **c.** Scatterplot demonstrating the association of ctDNA level with pack years of smoking for preoperative samples. Fitted line represents a linear model, and the shaded area represents the 95% confidence interval. **d.** Boxplot of preoperative ctDNA level for each pathological subtype of lung adenocarcinoma. The boxplots depict the median at the middle line, the lower and upper hinges represent the first and third quartiles, respectively, the whiskers show minima to maxima no greater than 1.5× the interquartile range (IQR), with the remaining

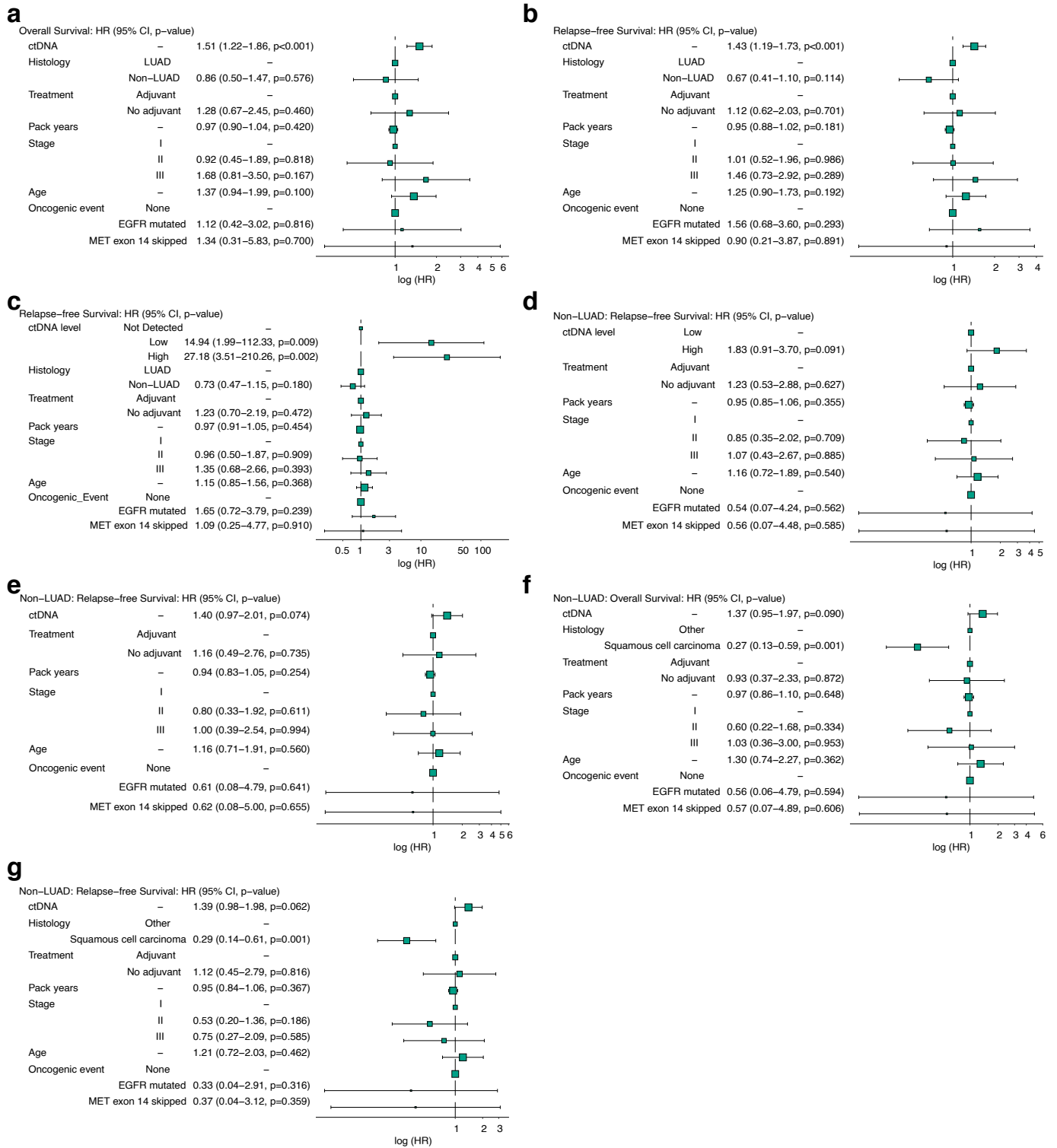
outlying data points plotted individually. Sample size is n = 94 patients. *P* value was calculated using two-sided Kruskal-Wallis rank sum test. **e.** Boxplot of preoperative ctDNA level by oncogenic event status. The boxplots depict the median at the middle line, the lower and upper hinges represent the first and third quartiles, respectively, the whiskers show minima to maxima no greater than 1.5× the IQR, with the remaining outlying data points plotted individually. Sample size is n = 171 patients. *P* value was calculated using two-sided Kruskal-Wallis rank sum test. **f.** Barplot of patient oncogenic event status colored by preoperative ctDNA detection status. *P* value was calculated using two-sided Fisher's exact test.



Extended Data Fig. 2 | See next page for caption.

Extended Data Fig. 2 | Increased assay sensitivity improves stratification of relapse-free survival. **a.** Kaplan–Meier (KM) curve demonstrating relapse-free survival (RFS) within ctDNA-high (dark grey), ctDNA-low (light grey) and ctDNA-negative (green) patients with lung adenocarcinoma. ctDNA high and low groups were defined according to the median ctDNA levels across ctDNA-positive LUADs. P values were calculated using log-rank tests. **b.** KM curve demonstrating

RFS within patients harbouring ctDNA at an estimated ppm below the limit of reliable detection described in Abbosh et al. 2023² (light grey), and ctDNA negative patients (green). P values were calculated using log-rank tests. **c.** KM curve illustrating difference in RFS between ctDNA-high and ctDNA-low patients with non-LUAD. P values were calculated using log-rank tests.

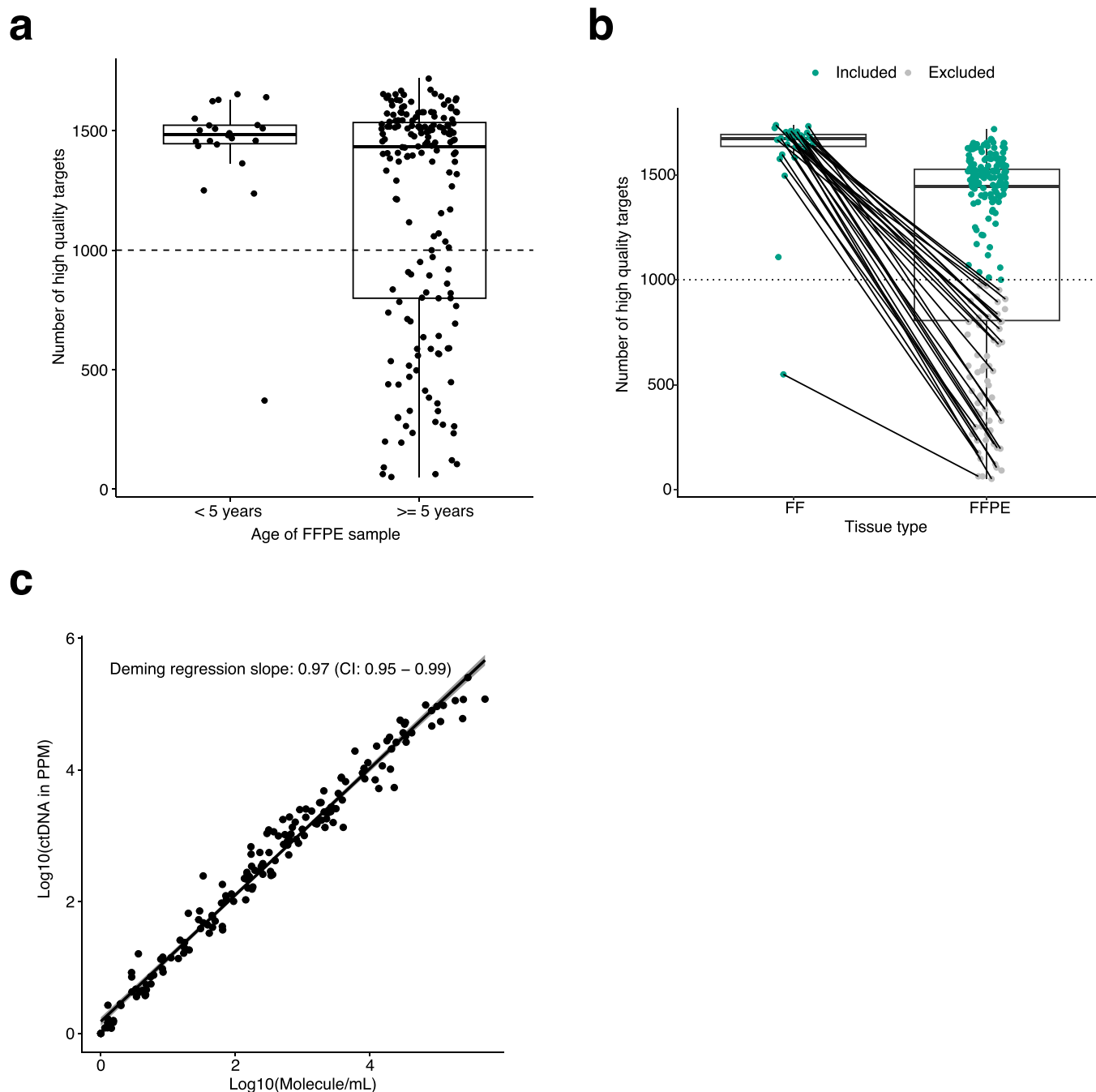


Extended Data Fig. 3 | See next page for caption.

Extended Data Fig. 3 | Multivariable analyses adjusting for known risk factors confirms independent prognostic value of pre-operative ctDNA.

a. Multivariable Cox regression analysis for overall survival (OS) containing ctDNA (continuous, per 10-fold increase); histology; whether the patient received adjuvant chemotherapy; cigarette smoking status (in 10 pack year increments); pTNM stage; age (in 10 year increments); and the presence of an oncogenic event. n = 171 patients. **b.** Multivariable Cox regression analysis for relapse-free survival (RFS) containing ctDNA (continuous, per 10-fold increase); histology; whether the patient received adjuvant chemotherapy; cigarette smoking history; pTNM stage; age; and the presence of an oncogenic event. n = 171 patients. **c.** Multivariable Cox regression analysis for RFS containing ctDNA level (ctDNA-high, ctDNA-low, ctDNA-negative); histology; whether the patient received adjuvant chemotherapy; cigarette smoking history; pTNM stage; age; and the presence of an oncogenic event. n = 171 patients. **d.** Multivariable Cox regression analysis for RFS in non-LUADs containing

ctDNA level (ctDNA-high, ctDNA-low); whether the patient received adjuvant chemotherapy; cigarette smoking history; pTNM stage; age; and oncogenic events. n = 77 patients. **e.** Multivariable Cox regression analysis for RFS in non-LUADs containing ctDNA (continuous); whether the patient received adjuvant chemotherapy; cigarette smoking history; pTNM stage; age; and oncogenic events. n = 77 patients. **f.** Multivariable Cox regression analysis for OS in non-LUADs containing ctDNA (continuous, per 10-fold increase); sub-histology; whether the patient received adjuvant chemotherapy; cigarette smoking history; pTNM stage; age and oncogenic events. n = 77 patients. **g.** Multivariable analysis for RFS in non-LUADs containing ctDNA (continuous, per 10-fold increase); sub-histology; whether the patient received adjuvant chemotherapy; cigarette smoking history; pTNM stage; age; and oncogenic events. n = 77 patients. For all plots in this figure, error bars represent 95% confidence intervals. The size of the boxes represents the number of patients within each category.



Extended Data Fig. 4 | The impact of sample age and preservation format on panel targets. **a.** Box and dot plot comparing number of high quality targets per panel from formalin-fixed paraffin embedded (FFPE) samples greater than 5 years vs less than 5 years old. Horizontal dashed line at 1000 indicates QC threshold. Center line represents the median. The upper whisker is the maximum value of the data that is within 1.5 times the interquartile range over the 75th percentile. The lower whisker is the minimum value of the data that is within 1.5 times the interquartile range under the 25th percentile. Sample size is $n = 202$. **b.** Failed FFPE or FFPE-derived panels which yielded fewer than 1000 high quality targets were re-generated using fresh frozen (FF) tissue where available. Green dots indicate samples included in our analysis, grey dots indicate those that failed to attain sufficient high quality targets for further processing. Where possible these panels were replaced with FF-derived panels. Connecting lines

indicate paired patient panels designed from either FF or FFPE tumor sample. Center line represents the median. The upper whisker is the maximum value of the data that is within 1.5 times the interquartile range over the 75th percentile. The lower whisker is the minimum value of the data that is within 1.5 times the interquartile range under the 25th percentile. Sample size is $n = 233$ panels. One panel constructed from an FF tumor sample failed to attain 1,000 high-quality targets but was included to ensure that the cohort was representative of the wider TRACERx cohort. Two FF panels were constructed where FFPE panels had failed altogether; these are represented by green dots on the FF side not connected to an FFPE dot. **c.** Deming regression demonstrating agreement between measured ctDNA PPM and tumor molecules per milliliter of plasma. Fitted line represents a linear model, and the shaded area represents the 95% confidence interval.

Reporting Summary

Nature Portfolio wishes to improve the reproducibility of the work that we publish. This form provides structure for consistency and transparency in reporting. For further information on Nature Portfolio policies, see our [Editorial Policies](#) and the [Editorial Policy Checklist](#).

Statistics

For all statistical analyses, confirm that the following items are present in the figure legend, table legend, main text, or Methods section.

- | n/a | Confirmed |
|-------------------------------------|--|
| <input type="checkbox"/> | <input checked="" type="checkbox"/> The exact sample size (n) for each experimental group/condition, given as a discrete number and unit of measurement |
| <input type="checkbox"/> | <input checked="" type="checkbox"/> A statement on whether measurements were taken from distinct samples or whether the same sample was measured repeatedly |
| <input type="checkbox"/> | <input checked="" type="checkbox"/> The statistical test(s) used AND whether they are one- or two-sided
<i>Only common tests should be described solely by name; describe more complex techniques in the Methods section.</i> |
| <input type="checkbox"/> | <input checked="" type="checkbox"/> A description of all covariates tested |
| <input type="checkbox"/> | <input checked="" type="checkbox"/> A description of any assumptions or corrections, such as tests of normality and adjustment for multiple comparisons |
| <input type="checkbox"/> | <input checked="" type="checkbox"/> A full description of the statistical parameters including central tendency (e.g. means) or other basic estimates (e.g. regression coefficient) AND variation (e.g. standard deviation) or associated estimates of uncertainty (e.g. confidence intervals) |
| <input type="checkbox"/> | <input checked="" type="checkbox"/> For null hypothesis testing, the test statistic (e.g. F , t , r) with confidence intervals, effect sizes, degrees of freedom and P value noted
<i>Give P values as exact values whenever suitable.</i> |
| <input checked="" type="checkbox"/> | <input type="checkbox"/> For Bayesian analysis, information on the choice of priors and Markov chain Monte Carlo settings |
| <input type="checkbox"/> | <input checked="" type="checkbox"/> For hierarchical and complex designs, identification of the appropriate level for tests and full reporting of outcomes |
| <input type="checkbox"/> | <input checked="" type="checkbox"/> Estimates of effect sizes (e.g. Cohen's d , Pearson's r), indicating how they were calculated |

Our web collection on [statistics for biologists](#) contains articles on many of the points above.

Software and code

Policy information about [availability of computer code](#)

Data collection	No software was used to collect data.
Data analysis	Personalis NeXT Personal Platform (v1.8) R version 4.1.3 R packages: tidyverse (version 1.3.2) lubridate (version 1.9.2) ComplexHeatmap (version 2.15.4) ggplot2 (version 3.4.2) ggpubr (version 0.4.0) scales (version 1.2.1) wesanderson (version 0.3.6) ggnewscale (version 0.4.9) survival (version 3.3-1) survminer (version 0.4.9) finalfit (version 1.0.4) gt (version 0.10.1) mcr (version 1.2.2)

All code needed to reproduce figures will be available on request.

For manuscripts utilizing custom algorithms or software that are central to the research but not yet described in published literature, software must be made available to editors and reviewers. We strongly encourage code deposition in a community repository (e.g. GitHub). See the Nature Portfolio [guidelines for submitting code & software](#) for further information.

Data

Policy information about [availability of data](#)

All manuscripts must include a [data availability statement](#). This statement should provide the following information, where applicable:

- Accession codes, unique identifiers, or web links for publicly available datasets
- A description of any restrictions on data availability
- For clinical datasets or third party data, please ensure that the statement adheres to our [policy](#)

Processed TRACERx patient data has been deposited at Zenodo at the link: 10.5281/zenodo.10689003. Raw data from TRACERx patients analyzed in this study including fastq and bam files from tumour and normal WGS, as well as fastq files from cfdNA have been deposited at the European Genome-phenome Archive (EGA), hosted by The European Bioinformatics Institute (EBI) and the Centre for Genomic Regulation (CRG) under accession codes (EGAS00001006494) under controlled access.

Research involving human participants, their data, or biological material

Policy information about studies with [human participants or human data](#). See also policy information about [sex, gender \(identity/presentation\), and sexual orientation](#) and [race, ethnicity and racism](#).

Reporting on sex and gender

Sex information has been included in the data shared online. Information on patients' gender was not collected as part of the study.

Reporting on race, ethnicity, or other socially relevant groupings

Information on race, ethnicity or other socially relevant groupings was not included in the manuscript.

Population characteristics

Cohort demographics (n =171) are included in Extended Data Table 1, and further patient-level details are available with supporting molecular data on Zenodo (link: 10.5281/zenodo.10689003). Inclusion and exclusion criteria for the TRACERx study (Clinical trial number: NCT01888601) are as follows:

Inclusion Criteria:
 Written Informed consent
 Patients ≥18 years of age, with early stage IIA-IIIb disease (according to TNM 8th edition) who are eligible for primary surgery.
 Patients with a radiological staging of IB (N0) who could be upstaged to IA-IIIb following surgery (due to the presence of possible nodal involvement on the pre-operative scan) may also be included, but will be withdrawn if post-surgical staging remains IB.
 Histopathologically confirmed NSCLC, or a strong suspicion of cancer on lung imaging necessitating surgery (e.g. diagnosis determined from frozen section in theatre)
 Primary surgery in keeping with NICE guidelines planned (see section 9.3)
 Agreement to be followed up at a TRACERx site
 Performance status 0 or 1
 Minimum tumour diameter at least 15mm to allow for sampling of at least two tumour regions (if 15mm, a high likelihood of nodal involvement on pre-operative imaging required to meet eligibility according to stage, i.e. T1N1-3)

Exclusion Criteria:
 Any other* malignancy diagnosed or relapsed at any time, which is currently being treated (including by hormonal therapy).
 Any other* current malignancy or malignancy diagnosed or relapsed within the past 3 years**.
 *Exceptions are: non-melanomatous skin cancer, stage 0 melanoma in situ, and in situ cervical cancer
 **An exception will be made for malignancies diagnosed or relapsed more than 2, but less than 3, years ago only if a pre-operative biopsy of the lung lesion has confirmed a diagnosis of NSCLC.
 Psychological condition that would preclude informed consent
 Treatment with neo-adjuvant therapy for current lung malignancy deemed necessary
 Post-surgery staging is not IIA-IIIb
 Known Human Immunodeficiency Virus (HIV), Hepatitis B Virus (HBV), Hepatitis C Virus (HCV) or syphilis infection.
 Sufficient tissue, i.e. a minimum of two tumour regions, is unlikely to be obtained for the study based on pre-operative imaging

Recruitment

When patients are initially diagnosed with stage I-III lung cancer and then referred for surgical resection, a research nurse identifies them on a clinic/operating list. The patient has an initial eligibility assessment and is then provided with written information about the TRACERx study and he/she can ask the research nurse any questions.

Patients have to agree to provide serial blood samples whenever they attend clinic for routine blood sampling, so this represents the only main potential self-selecting bias (i.e. only patients willing to do this would participate). However, it is unclear how this would affect the biomarker analyses. Also, the gender and ethnicity characteristics are in line with patients seen in routine practice.

Ethics oversight

This study was approved by the NRES Committee London with the following details:
 Study title: TRACing non small cell lung Cancer Evolution through therapy (Rx)

REC reference: 13/LO/1546
 Protocol number: UCL/12/0279
 IRAS project ID: 138871
 Written informed consent was obtained from all participants.

Note that full information on the approval of the study protocol must also be provided in the manuscript.

Field-specific reporting

Please select the one below that is the best fit for your research. If you are not sure, read the appropriate sections before making your selection.

Life sciences Behavioural & social sciences Ecological, evolutionary & environmental sciences

For a reference copy of the document with all sections, see [nature.com/documents/nr-reporting-summary-flat.pdf](https://www.nature.com/documents/nr-reporting-summary-flat.pdf)

Life sciences study design

All studies must disclose on these points even when the disclosure is negative.

Sample size	Here, we report analyses from 204 TRACERx patients. No sample size calculations were performed for the preoperative ctDNA substudy; sample size was determined by sample availability, and includes 18 patients from the Abbosh et al., 2017 study and 43 patients from the Abbosh et al., 2023 study. Tumor / normal WGS for 171 patients yielded passing ctDNA panels that were included for further analysis. 171 patients had preoperative plasma available, including 89 patients who had disease relapse.
Data exclusions	Patients were excluded if they did not have baseline plasma. The available plasma collected at or closest to surgery was included in the analyses for patients with multiple pre-surgical plasma. We obtained FFPE tissue for 204 patients. Of these, 62 had atypically low counts of high quality panel targets (<1,000) likely due to age and/or poor quality of the FFPE samples, and 2 did not pass panel design. For 31 of these 64 patients, DNA extracted from fresh frozen tissue was available and the remaining 33 patients were excluded from analysis.
Replication	In-silico and technical replicates were used for analytical validation of the NeXT Personal Platform. Supporting experiments are described in both the main body of the manuscript as well as in the methods, and are visualized in Figure 1 and Extended Data Figure 1.
Randomization	No randomization was performed in the this study as no therapeutic interventions are tested.
Blinding	Retrospective ctDNA analysis was conducted using prospectively collected specimens and clinical follow up. Personalis investigators were fully blinded to patient clinical outcome and clinical pathological characteristics during sample processing and ctDNA analysis. Likewise, TRACERx investigators were blinded to patient ctDNA status during clinical data and patient specimen collection.

Reporting for specific materials, systems and methods

We require information from authors about some types of materials, experimental systems and methods used in many studies. Here, indicate whether each material, system or method listed is relevant to your study. If you are not sure if a list item applies to your research, read the appropriate section before selecting a response.

Materials & experimental systems

n/a	Involvement in the study
<input checked="" type="checkbox"/>	<input type="checkbox"/> Antibodies
<input type="checkbox"/>	<input checked="" type="checkbox"/> Eukaryotic cell lines
<input checked="" type="checkbox"/>	<input type="checkbox"/> Palaeontology and archaeology
<input checked="" type="checkbox"/>	<input type="checkbox"/> Animals and other organisms
<input type="checkbox"/>	<input checked="" type="checkbox"/> Clinical data
<input checked="" type="checkbox"/>	<input type="checkbox"/> Dual use research of concern
<input checked="" type="checkbox"/>	<input type="checkbox"/> Plants

Methods

n/a	Involvement in the study
<input checked="" type="checkbox"/>	<input type="checkbox"/> ChIP-seq
<input checked="" type="checkbox"/>	<input type="checkbox"/> Flow cytometry
<input checked="" type="checkbox"/>	<input type="checkbox"/> MRI-based neuroimaging

Eukaryotic cell lines

Policy information about [cell lines and Sex and Gender in Research](#)

Cell line source(s)	NA
Authentication	As provided by ATCC (STR profiling).
Mycoplasma contamination	Examined by ATCC and confirmed as not detected.
Commonly misidentified lines (See ICLAC register)	None of these are commonly misidentified cell lines as reported by the ICLAC register.

Clinical data

Policy information about [clinical studies](#)

All manuscripts should comply with the ICMJE [guidelines for publication of clinical research](#) and a completed [CONSORT checklist](#) must be included with all submissions.

Clinical trial registration	TRACERx Non-small Cell Lung Cancer Evolution Through Therapy (Rx) (TRACERx): https://clinicaltrials.gov/study/NCT01888601
Study protocol	https://clinicaltrials.gov/study/NCT01888601
Data collection	Clinical and pathological data is collected from patients during study follow up - this period is a minimum of five years. Data collection is overseen by the sponsor of the study (Cancer Research UK & UCL Cancer Trials Centre) and takes place in hospitals across the United Kingdom. A centralised database called MACRO is used for this purpose. Recruitment to TRACERx started in April 2014 and is ongoing.
Outcomes	<p>The pre-defined clinical outcome analysed in this manuscript is overall survival (OS) measured from the time of study registration to date of death from any cause. This outcome was previously defined in the TRACERx protocol (described in Jamal-Hanjani et al., 2017 NEJM). Additional analysis of relapse-free survival is also included in this manuscript, and is defined as the days from registration to any disease recurrence or new primary tumor events. The primary and secondary outcomes were pre-defined based on the following primary and secondary study objectives:</p> <p>Primary objectives: Define the relationship between intratumour heterogeneity and clinical outcome (disease-free survival and overall survival) following surgery and adjuvant therapy (including relationships between intratumour heterogeneity and clinical disease stage and histological subtypes of NSCLC).</p> <p>Establish the impact of adjuvant platinum-containing regimens upon intratumour heterogeneity in relapsed disease compared to primary resected tumour.</p> <p>Secondary objectives: Development and validation of an intratumour heterogeneity ratio index as a prognostic or predictive biomarker in relation to its association with DFS and OS</p> <p>Infer a complete picture of NSCLC evolutionary dynamics: Define drivers of genomic instability, metastatic progression and drug resistance by identifying and tracking the dynamics of somatic mutational heterogeneity, and chromosomal structural and numerical instability present in the primary tumour and at metastatic sites. Individual tumour phylogenetic tree analysis will:</p> <ol style="list-style-type: none">Establish the order of somatic events in relation to genomic instability onset and metastatic progressionDecipher genetic “bottlenecking” events following metastasis and drug therapyEstablish dynamics of tumour evolution during the disease course from early to late stage NSCLC. <p>Initiate a longitudinal minimally-invasive circulating tumour cells (CTC) and cfDNA biobank to develop analytical methods for the early detection and monitoring of tumour evolution over time.</p> <p>Develop a longitudinal tissue resource to serve as a platform to assess the relationship between genetic intratumour heterogeneity and the host immune response.</p> <p>Isolate monocytes and lymphocytes for the in vitro generation of neoantigen-reactive T cells to be tested for immunoreactivity to matched tumour samples</p> <p>Develop a repository of lung cancer cell lines, organoids and in vivo mouse models of patient- derived lung cancers that can be used as in vitro and in vivo models to study the aetiology of lung diseases, including lung cancer and predict response to therapeutics and resistance in lung cancer.</p> <p>Define relationships between intratumour heterogeneity and targeted/cytotoxic therapeutic outcome.</p> <p>Through UCL-GCLP gene panel in a certified laboratory environment, TRACERx will define clonally dominant disease drivers (paired primary-metastatic site comparisons in at least 270 patients with relapsed disease) to address the role of clonal driver dominance in targeted therapeutic response, and to guide stratification of lung cancer treatment and future clinical study inclusion in collaboration with the CRUK Stratified Medicines Phase II program.</p> <p>Develop analytical methods for determining morphological heterogeneity within separate tumour regions.</p>

Tissue samples obtained from lung resections, both tumour and normal, will be analysed using high-power microscopy, such as electron microscopy, in order to obtain information regarding cellular structures.

The work presented in this manuscript assessed the impact of ctDNA on patient survival via Cox regression analysis and the Kaplan Meier method.